Towards (C,C)-cyclometalated N -(9-alkylfluorenyl)NHC Ruthenium Complexes for Z -selective Olefin Metathesis

Katarzyna Gajda, Adrian Sytniczuk, Laure Vendier, Bartosz Trzaskowski, Noël Lugan, Anna Kajetanowicz, Stéphanie Bastin, Karol Grela, Vincent César

▶ **To cite this version:**

Katarzyna Gajda, Adrian Sytniczuk, Laure Vendier, Bartosz Trzaskowski, Noël Lugan, et al.. Towards (C,C)-cyclometalated N -(9-alkylfluorenyl)NHC Ruthenium Complexes for Z -selective Olefin Metathesis. European Journal of Inorganic Chemistry, 2023, 26 (20), pp.e202300169. 10.1002/ejic.202300169 . hal-04155197

HAL Id: hal-04155197
https://hal.science/hal-04155197

Submitted on 7 Jul 2023

HAL is a multi-disciplinary open access archive for the deposit and dissemination of scientific research documents, whether they are published or not. The documents may come from teaching and research institutions in France or abroad, or from public or private research centers.

L'archive ouverte pluridisciplinaire **HAL**, est destinée au dépôt et à la diffusion de documents scientifiques de niveau recherche, publiés ou non, émanant des établissements d'enseignement et de recherche français ou étrangers, des laboratoires publics ou privés.

Towards (*C,C*)-cyclometalated *N*-(9-alkylfluorenyl)NHC ruthenium complexes for *Z*-selective olefin metathesis

Katarzyna Gajda,[a,b] Adrian Sytniczuk,[b] Laure Vendier,[a] Bartosz Trzaskowski,[c] Noël Lugan,[a] Anna Kajetanowicz,*[b] Stéphanie Bastin,*[a] Karol Grela,*[b] Vincent César*[a]

[a] K. Gajda, Dr. L. Vendier, Dr. N. Lugan, Dr. S. Bastin, Dr. V. César
LCC-CNRS
Université de Toulouse, CNRS
205 route de Narbonne. 31077 Toulouse cedex 4, France
E-mail: stephanie.bastin@lcc-toulouse.fr
vincent.cesar@lcc-toulouse.fr

[b] K. Gajda, Dr. A. Sytniczuk, Dr. A. Kajetanowicz, Prof. K. Grela
Biological and Chemical Research Centre, Faculty of Chemistry
University of Warsaw
Żwirki i Wigury Street 101
02-089 Warsaw, Poland
E-mail: a.kajetanowicz@uw.edu.pl
prof.grela@gmail.com

[c] Prof. B. Trzaskowski
Centre of New Technologies
University of Warsaw
S. Banacha 2c
02-097 Warsaw, Poland

Supporting information for this article is given via a link at the end of the document.((Please delete this text if not appropriate))

Abstract: Three Hoveyda-Grubbs complexes supported by *N*-(9-alkylfluorenyl)imidazol-2-ylidene ligands (alkyl = methyl, ethyl or benzyl) have been synthesized. With the aim to generate chelating, cyclometalated (C,C_{NHC}) ruthenium complexes for *Z*-selective olefin metathesis, the C(sp^3)-H activation of the dangling alkyl group has been studied. While the methyl derivative leads to the expected cyclometalated complex, a C(sp^2)-H activation of the fluorenyl moiety and no evolution/transformation are observed for the ethyl and benzyl derivatives, respectively. Although highly fragile under catalytic conditions, the cyclometalated complex leads to *Z/E* stereoselectivity up to 94/6. An unprecedented insertion of the alkylidene moiety into the Ru-C_{NHC} bond leading to ruthenium N-heterocyclic olefin complexes is also observed and supported by calculations of the corresponding reaction pathway.

Introduction

Olefin metathesis offers a unique, atom-efficient catalytic route towards carbon-carbon double bonds and has imposed over the years as a prominent synthetic methodology in contexts ranging from natural products and pharmaceuticals synthesis to materials science.[1] Besides molybdenum-, tungsten-, and vanadium-based catalysts,[2] a plethora of well-defined ruthenium olefin metathesis catalysts has been developed since the 1990's thanks to their broad functional group tolerance and good stability against air and moisture.[3] Whereas the efficiency, substrate scope or chemoselectivity of the catalysts could be optimized in many cases, the stereoselectivity control remains a great challenge and *E/Z* mixtures of alkene products are typically generated. As olefin metathesis is by nature under thermodynamic control, the *E/Z* distribution indeed reflects the relative stabilities of the two isomers, which is usually in favor of the more stable *E* isomers.

The development of efficient *Z*-selective olefin metathesis catalysts, which kinetically enable selective synthesis of *Z*-(*cis*) isomers, has only been achieved in the last decade and still remains a big challenge (Figure 1).[4] In 2011, Schrock and Hoveyda reported the first successful example based on the bulky monoaryloxide pyrrolide Mo complex **A**.[5] Soon after, Grubbs disclosed the family of ruthenium complexes **B**, whose key features are a (*C,C*)-cyclometalated N-adamantyl-NHC and a chelating LX-type ligand such as pivalate or nitrate.[6] A second family of Z-selective Ru-based metathesis catalysts **C** supported by a highly hindered monothiolate ligands was discovered by Jensen and Occhipinti two years later.[7] Eventually, the dithiolate ruthenium complexes **D** constitute the main family of stereoretentive olefin metathesis catalysts, i.e. the stereochemistry of the alkene substrate is transferred to the alkene product.[8],[9]

Grubbs-type complexes **B** were shown to be the most efficient and general in Z-selective metathesis catalysis and were the subject of structure/stability/activity relationship studies.[6b, 6d, 6f, 6g] 5-membered metallacycles are preferentially generated compared to 4 and 6-membered ones and the steric hindrance around the chelating alkyl ligand plays a crucial role for the stability and activity of the catalysts, with the *N*-(adamant-1-yl) substituent constituting the best compromise.[6f]

Due to its high steric hindrance and rigidity, the *N*-(fluoren-9-yl) substituent imposes a specific conformation to the NHC ligand in complexes **E**, in which the hydrogen atom in the fluorenyl- 9 position is pointing towards the metal center.[10],[11] This specific feature was leveraged to create extremely bulky "hummingbird" *N,N'*-(9-alkylfluorenyl)NHC complexes **F**, in which the two alkyl chains embrace the metal center.[12] Based on these structural considerations, we thus devised to develop Hoveyda-type complexes **G** supported by a *N*-(9-alkylfluorenyl)NHC ligand and study the possibility to generate the corresponding cyclometalated complexes of type **H**. We report herein the synthesis, characterization and catalytic activities of a series of three complexes **G** by varying the alkyl chain from the methyl (R_1=H) to ethyl (R_1 = Me) and benzyl (R_1 = Ph) groups, as well as

the outcome of their cyclometalation, which greatly depends on the nature of the alkyl chain. In addition, an original and clean migration reaction of the NHC ligand induced by the addition of silver salt is reported.

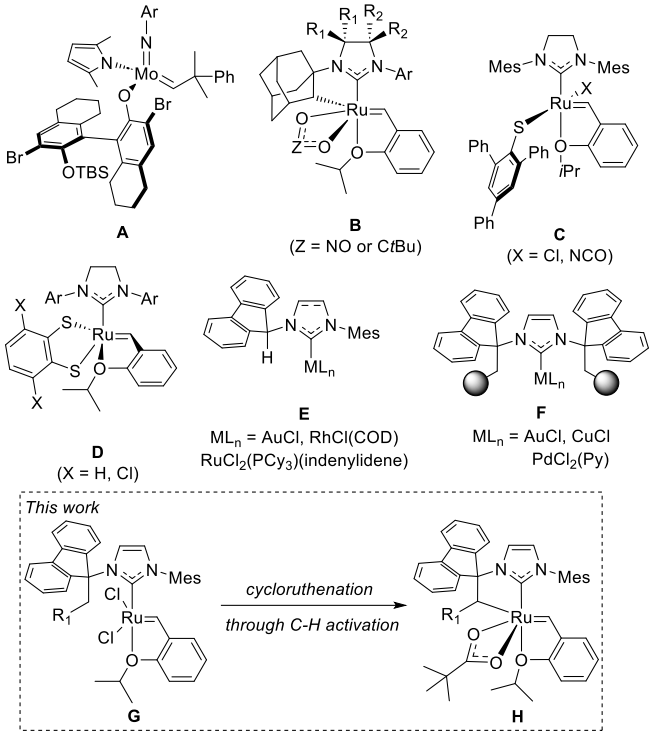

Figure 1. Examples of Z-selective (**A-C**) and stereoretentive (**D**) Ru olefin metathesis catalysts. Previously reported N-(fluorenyl)NHC complexes **E** and **F** and target complexes **G** and **H** in this study.

Results and Discussion

Synthesis of the Hoveyda-type second-generation complexes

Three *N*-(9-alkylfluorenyl)imidazolium tetrafluoroborate salts **2a-c**·HBF_4 were synthesized, where the alkyl R group is a methyl (**a**), an ethyl (**b**) or a benzyl (**c**) group. They were obtained by selective alkylation of the fluorenyl position starting from the parent unsubstituted *N*-fluorenyl-N'-mesitylimidazolium bromide **1**·HBr according to a procedure previously reported by some of us (Scheme 1).[10] **1**·HBr was selectively mono-deprotonated using potassium bis(trimethylsilyl)amide (KHMDS) as a strong base resulting in the formation of the bright yellow mesoionic N-ylide **1**, whose fluorenyl position could be alkylated by adding methyl iodide, ethyl bromide or benzyl bromide to generate **2a-c**·HX, respectively. After anion metathesis, the *N*-(9-alkylfluorenyl)imidazolium tetrafluoroborate salts **2a-c**·HBF_4 were isolated in 81, 77 and 76% yields, respectively. Although efficient, this synthesis required to be performed in dry solvents and under an inert gas atmosphere because of the sensitivity of zwitterion **1** towards air and moisture. We thus developed the new alkylating route b, in which the starting imidazolium **1**·HBr was reacted *in situ* with potassium carbonate as a mild and selective base and the alkylating reagent, in acetonitrile, followed by an anion metathesis step. This procedure allowed the practical and efficient synthesis of **2b-c**·HBF_4 akin to the previous one. However, no alkylation was observed when methyl iodide was used as the alkylating agent following this route, probably due to competitive methylation of the carbonate anion with methyl iodide. Deprotonation of the imidazolium salts **2a-c**·HBF_4 with potassium *tert*-amylate (*t*-AmOK) in hexane followed by the addition of Hoveyda-Grubbs 1st generation complex $RuCl_2(PCy_3)$[=CH(*o*-*i*PrO-Ph)] (**Hov-I**) yielded the corresponding Hoveyda-Grubbs 2nd generation complexes **3a-c** in 65-76% yields through displacement of PCy_3 by the NHCs **2a-c** generated *in situ*. The use of hexane is critical in this complexation, as only low yields of the complexes (~25%) were observed when the reaction was carried out in toluene. Indeed, the complexes **3a-c** being not soluble in hexane, they precipitated during the course of the reaction shifting the equilibrium towards products and as solids, they were less prone to decompose.

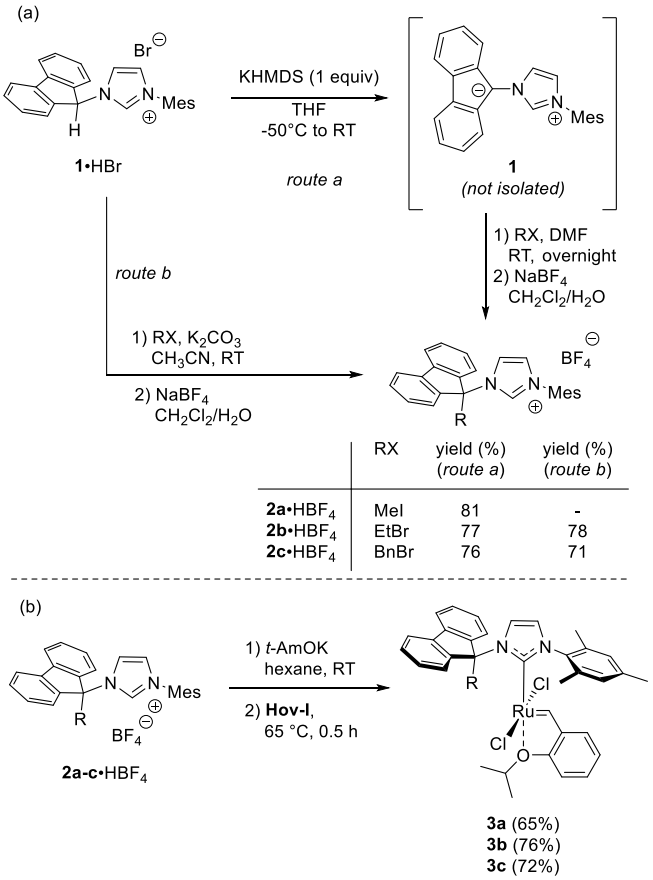

Scheme 1. (a) Synthesis of the N-(9-alkylfluorenyl)imidazolium salts **2a-c**·HBF_4. (b) Synthesis of the corresponding Hoveyda-type complexes **3a-b** supported by *N*-(9-alkylfluorenyl)NHC ligands **2a-c.** Mes = 2,4,6-trimethylphenyl. **Hov-I** = $RuCl_2(PCy_3)$[=CH(*o*-*i*PrO-Ph)].

After filtration of the reaction mixture and purification by column chromatography, complexes **3a-c** were isolated as green microcrystalline solids. The new complexes were fully characterized by spectroscopic and analytical methods, supplemented by single-crystal X-ray diffraction analyses (Figure 2). The NMR spectroscopic data of complexes **3a-c** agreed with the proposed structures. The characteristic signals of the benzylidene Ru=C*H* protons were observed at δ = 17.05, 17.08, and 17.08 ppm, while the benzylidene carbon atoms Ru=*C*H resonate at δ = 307.6, 307.2, and 307.8 ppm for **3a**, **3b** and **3c**, respectively. Most importantly, the complexation reaction exerted a significant effect on the fluorenyl methyl protons in **3a** and of the methylene CH_2 protons in **3b-c**, whose signals are particularly low-field shifted with respect to the corresponding ones in the

starting imidazolium salts **2a-c**·HBF_4 [$\Delta\delta$ = 1.84 ppm (**3a**), 2.33 ppm (**3b**), 2.47 ppm (**3c**)]. This behavior, previously observed to a lower extent upon complexation in complexes of type **F**,[12a, 12d] strongly indicated binding interactions between the methylic-(**3a**) or methylenic-H atoms (**3b-c**) and the ruthenium center.

This was corroborated by the analysis of the molecular structures of **3a-c** in the solid state (Figure 2 and Table 1).[13]

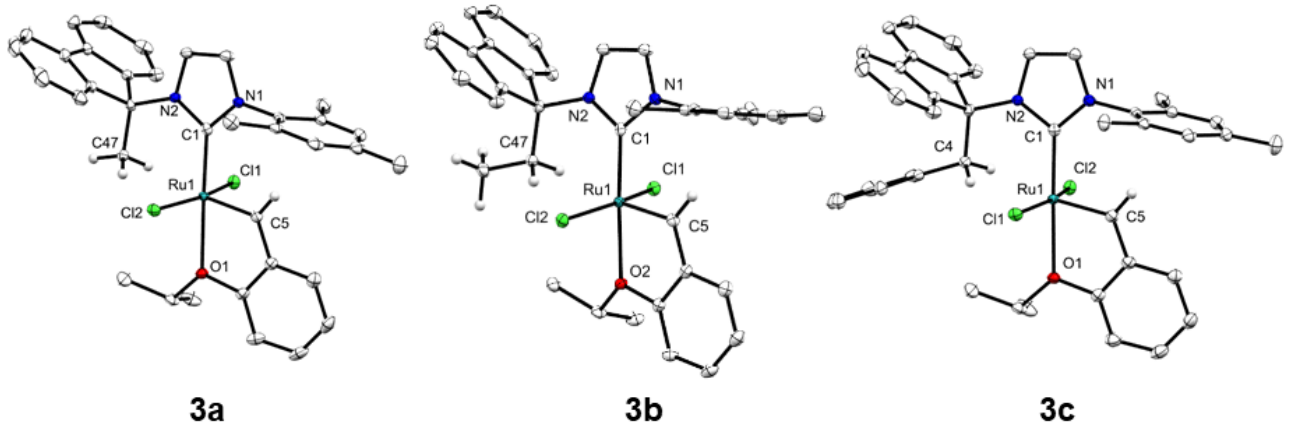

Figure 2. Molecular structures of complexes **3a** (left), **3b** (center), and **3c** (right) (ellipsoids drawn at 30% probability level). Solvent and hydrogen atoms, except on the benzylidene moiety and on the fluorenyl methyl (**3a**), ethyl (**3b**), and methylene group (**3b**), have been omitted for clarity.

Table 1. Selected bond lengths (Å) and angles (deg) for complexes **3a-c**.

3a		**3b**]		**3c**	
Ru1-C1	1.989(2)	Ru1-C1	1.9952(13)	Ru1-C1	1.9978(17)
Ru1-C5	1.835(2)	Ru1-C5	1.8362(13)	Ru1-C5	1.8410(18)
Ru1-O1	2.2942(16)	Ru1-O2	2.2710(9)	Ru1-O1	2.2961(12)
Ru1-C47	2.847	Ru1-C47	2.953	Ru1-C4	2.842
C1-Ru1-O1	177.95(8)	C1-Ru1-O2	175.27(4)	C1-Ru1-O1	177.20(6)
C1-Ru1-C5	100.89(10)	C1-Ru1-C5	100.95(5)	C1-Ru1-C5	101.14(7)
Cl1-Ru1-Cl2	164.175(19)	Cl1-Ru1-Cl2	162.155(12)	Cl1-Ru1-Cl2	164.220(15)

All three complexes exhibit a pentacoordinate ruthenium center within a distorted square pyramidal geometry characterized by a geometry index τ_5 = 0.23 (**3a**), 0.22 (**3b**) and 0.22 (**3c**),[14] the benzylidene ligand occupying the apex of the pyramid. In all three complexes, the *N*-fluorenyl arm is located on the opposite side to the benzylidene moiety placing its alkyl substituent in the open space of the coordination sphere and in close proximity to the ruthenium center. The distances between the ruthenium center and the first carbon atom of the alkyl chain [Ru1-C47: 2.847 Å for **3a**, Ru1-C47: 2.953 Å for **3b**, Ru1-C4: 2.842 Å for **3c**] are rather similar to the one recorded in Hoveyda-II complexes bearing *N*-adamantyl NHC ligands [2.804-2.886 Å],[6a, 6g] precursors for cyclometalated complexes **B**. As a consequence of this specific spatial arrangement, a steric repulsion is observed with the two *trans*-disposed chloride ligands and the Cl1-Ru1-Cl2 angles in **3a-c** [162.155° – 164.220°] are greater of about 8 degrees than the Cl-Ru-Cl angles in the majority of reported Hoveyda-type ruthenium complexes bearing unsymmetrical NHC ligands.[11b, 15] Other structural parameters are otherwise classical for Hoveyda-type second generation complexes.

Thermal stability and olefin metathesis catalytic activity studies of complexes 3a-c

The thermal stabilities of complexes **3a-c** were evaluated using a standardized procedure. The commercially available Hoveyda-Grubbs second-generation catalyst **Hov-II** [Hov-II = $RuCl_2$(SIMes)(=CH(*o*-O*i*Pr)Ph)] was added to this test as reference, since it is a general-purpose catalyst bearing the symmetrical SIMes ligand (SIMes = 1,3-dimesitylimidazolidin-2-ylidene). Hence, samples of the corresponding catalysts and 1,3,5-trimethoxybenzene (used as an internal standard) were carefully weighed in a glove box, dissolved in toluene-d_8 (0.7 mL) and placed in Young-tap NMR tubes, which were heated at 50°C for several days. The ^{1}H NMR spectra were recorded and the degree of degradation of the catalyst was determined based on the integration of the benzylidene signal of the complexes (peaks in the range of 16-17 ppm) and methoxy groups (6.15 ppm) of the internal standard (Figure 3). While the **Hov-II** catalyst remained intact after 6 days at 50°C, a net decomposition of complexes **3a-c** was observed during the same period and only 77, 69, and 78% of **3a-c**, respectively, were still present after 6 days.

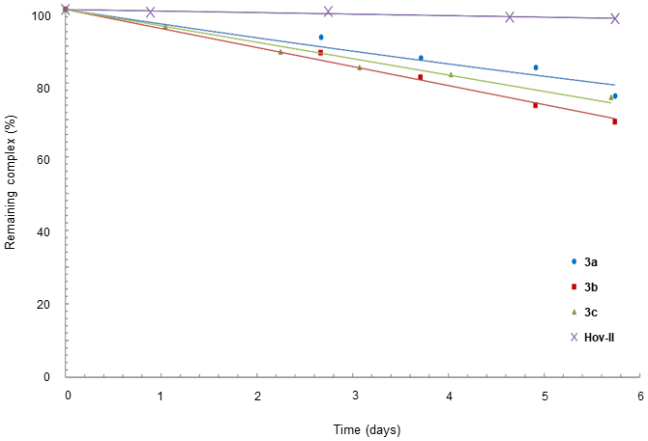

Figure 3. Stability tests of Hoveyda-type complexes **3a-c** and **Hov-II** in toluene-d_8 at 50 °C under argon. Monitored by ^{1}H NMR spectroscopy using 1,3,5-trimethoxybenzene as internal standard. Lines placed as visual aids.

The activity of complexes **3a-c** in model olefin metathesis reactions was then investigated. As an initial evaluation on relatively undemanding substrates, the RCM reaction of the most commonly used model diene,[16] diethyl diallylmalonate (**4**) was examined using 1 mol% of catalyst (Figure 4). Initially the reaction was carried out at 50°C, at which **Hov-II** achieved full conversion into **5** after only 3 minutes. All three catalysts **3a-c** were much less efficient and conversions did not exceed 40% threshold even after 90 min. The reaction still proceeded even after 90 min reaction time, as there is no visible plateau, but at a very low rate. To investigate the influence of the temperature, the latter was increased to 80°C after 70 min during the reaction carried out in the presence of **3a**. A small leap in conversion was observed, which prompted us to perform the reaction at 80°C. Unfortunately, while the initial rates were found to be approximately 9 times higher than at 50°C, a rapid decomposition of the catalysts **3a-c** was apparent and after 15 min, a plateau was reached at 31% conversion for **3b**, and 22% conversion for both **3a** and **3c**. Additionally, the catalysts **3a-c** were shown to be almost inactive at room temperature.

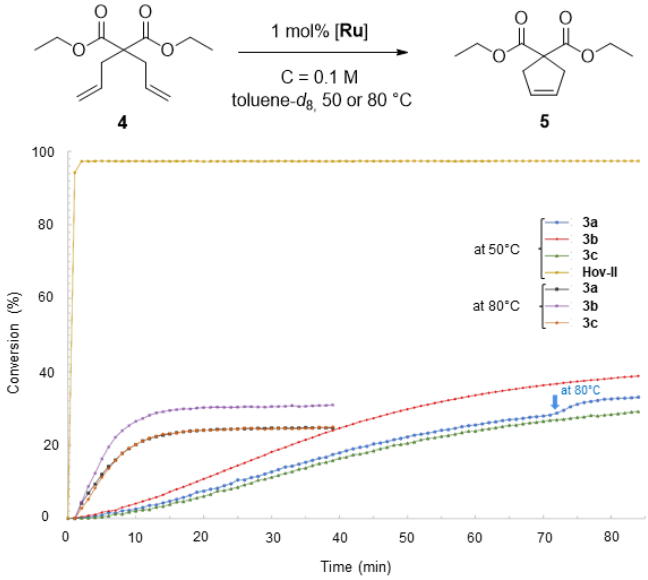

Figure 4. Time/conversion curves for the RCM reaction of DEDAM with 1 mol% of Ru complexes at 50°C and 80°C (monitored by ^{1}H NMR). Lines are visual aids only. **Hov-II** = $RuCl_2$(SIMes)[=CH(*o*-*i*PrO-Ph)].

Synthesis of the cyclometalated ruthenium complexes

Complex **3a** was used as the model substrate for the development and optimization of the cyclometallation conditions. The experiments were carried out in Young-tap NMR tubes to directly follow the course of the reaction. Grubbs' original conditions, namely 2 equivalents of silver pivalate (AgOPiv) in THF-d_8,[6a] were first screened. Unfortunately, monitoring of the reaction at room temperature by ^{1}H NMR revealed no additional benzylidene signal and led to a rather rapid decomposition of complex **3a** into an intractable mixture. We therefore turned our attention to a milder method, employing sodium pivalate (NaOPiv) instead of AgOPiv, and which had already been reported to provide access to a range of cyclometalated metathesis catalysts.[6f] When mixing complex **3a** with a large excess of NaOPiv in MeOH-d_4, we were pleased to observe the appearance of an additional benzylidene signal in the low-field region in ^{1}H NMR. The reaction was completed within 7 hours at 50°C. Encouraged by this result, we performed the reaction on a synthetic scale (~0.3 mmol) using 15 equivalents of NaOPiv in a THF/MeOH solvent mixture (Scheme 2). After treatment and crystallization, the target cyclometalated complex **6a** was isolated in 42% yield as purple crystals, along with the side-product **6a'** isolated in 8% yield as a yellow powder.

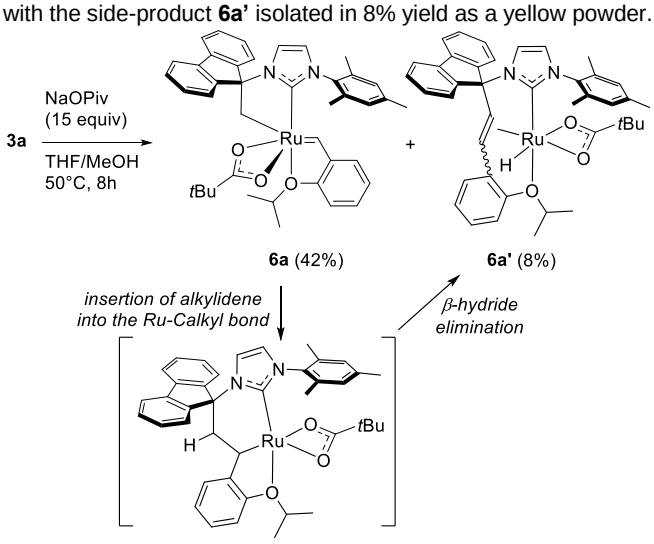

Scheme 2. Synthesis of the cyclometalated complex **6a** and by-product **6a'**, and the postulated mechanism of decomposition of complex **6a**.

Complex **6a** is highly sensitive to air and moisture even in the solid state and should be kept in a glove box. It was characterized by multinuclear, multidimensional NMR experiments, HRMS and its molecular structure was firmly established by an X-Ray diffraction experiment on a single crystal. While complex **3a** had a C_s-symmetry, ^{1}H and ^{13}C NMR spectra of **6a** were consistent with a C_1-symmetry. As expected, the benzylidene signal was upfield-shifted compared to the corresponding signal in **3a** and was observed at δ = 15.74 ppm. The cyclometalation was confirmed by the presence of two doublets at δ = 4.01 and 3.21 ppm ($^2J_{HH}$ = 11.7 Hz) corresponding to the diastereotopic CH_2 protons of the (fluoren-9-yl)methyl ligand in the ^{1}H NMR spectrum and by the

downfield-shifted resonance of the CH_2 carbon atom at δ = 42.5 ppm in the ^{13}C NMR spectrum.

Complex **6a** crystallized as a racemate in the centrosymmetric $C_{2/c}$ space group (Figure 5). Its molecular structure was found to be rather similar to the previously reported structures of type **B**,[6a, 6g] i.e. an 18e-complex with a distorted octahedral geometry, in which the alkyl, benzylidene and chelating pivalate ligands are in the same coordination plane. The coordination sphere is completed by the NHC and the ether ligands, which are in *trans* position. The Ru1-C1 bond length of 1.948(3) Å is slightly shorter than the corresponding Ru1-C1 in **3a** [1.989(2) Å] and this could be ascribed to the formation of the 5-membered ruthenacycle, that induced greater structure strain. Although the chelating *N*-(9-methylfluorenyl) arm in **6a** is of different nature compared to the *N*-(adamantyl) arm in complexes **B**, the Ru1-C26 bond length of 2.072(3) Å is similar to the Ru-$C_{(Ad-2)}$ in **B** [2.053(4)-2.065(3) Å].

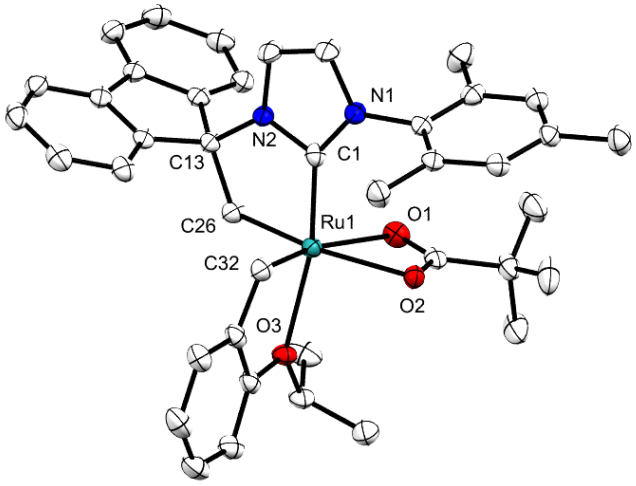

Figure 5. Molecular structure of **6a**. Ellipsoids drawn at the 30% probability level. Hydrogen atoms and solvent molecules were omitted for clarity. Selected bond distances (Å) and angles (deg): Ru1-C1 1.948(3), Ru1-C26 2.072(3), Ru1-C32 1.858(3), C1-Ru1-C26 80.60(11), C1-Ru1-C32 92.37(12), C26-Ru1-C32 95.38(12).

Although no single crystals of the side-product **6a'** could be grown for an X-Ray diffraction experiment, its molecular structure could be established by multidimensional NMR spectroscopy and HRMS experiments. Noteworthy is the presence of a coordinated alkene moiety, characterized by a set of two doublets in ^1H NMR at δ = 4.05 and 3.31 ppm with a coupling constant of 7.5 Hz and by the corresponding ^{13}C resonances at δ = 75.5 and 64.6 ppm in the ^{13}C NMR spectrum, but the *E/Z* configuration could not be firmly established with these data.[17] From the 2D NMR correlation experiments, we could also established that the alkene moiety connects the fluorenyl part of the NHC ligand with the o-(isopropoxy)phenyl group. More importantly, the characteristic singlet at δ = – 9.94 ppm in ^1H NMR spectrum indicated a ruthenium hydride moiety. Eventually, a pivalate molecule completed the coordination sphere of complex **6a'**, which could be formulated as the saturated, 18e octahedral complex depicted in Scheme 2. According to Houk and Grubbs,[18] the Ru-H complex **6a'** might arise here from the decomposition of the cyclometalated complex **6a** by insertion of the alkylidene moiety into the ruthenium-alkyl bond followed by a β-H elimination (Scheme 2).

Encouraged by the obtention of the cyclometalated complex **6a**, the intramolecular cyclometallation of the ethyl- and benzyl-derivatives **3b** and **3c** was attempted by using the same reaction conditions. In the case of **3c**, despite longer reaction time and higher temperature, no additional benzylidene signal appeared in the ^1H NMR spectrum of the crude reaction mixture, suggesting that **3c** is reluctant to cyclometallation, most probably due to steric constraints. Conversely, the benzylidene signal of **3b** disappeared during the reaction, which was accompanied by the appearance of a broad signal and of a small additional signal in the downfield region. After 8 hours, the reaction was worked up as before and crystallization of the crude product resulted in green crystals and a tiny amount of a purple solid. While the exact nature of the purple solid could not be firmly established, an X-Ray diffraction analysis of the green crystals indicated that they correspond to the complex **7b**, which was isolated in 48% (Scheme 3).

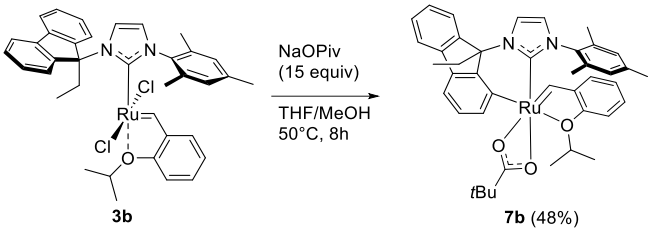

Scheme 3. Synthesis of the cyclometalated complex **7b**.

Complex **7b** crystallized in the orthorhombic Pbca space group (Figure 6). It consists of a cyclometalated complex with a distorted octahedral geometry around the Ru center. Surprisingly, the cyclometallation did not occur at the C(sp^3)-H bond of the dandling ethyl substituent but at a C(sp^2)-H position of the fluorenyl moiety, leading to a 6-membered metallacycle. Contrary to previous cyclometalated alkylidene complexes, the ether function of the *o*-(isopropoxy)benzylidene ligand is not in *trans* position but in *cis* position relative to the NHC ligand, as is the case with the benzylidene. One of the oxygen atoms of the chelating pivalate ligand is placed in *trans* position relative to the NHC. More surprising is the rather long Ru1-C1 of 2.0767(18) Å compared to the Ru1-C1 in **3b** [1.9952(13) Å] and even compared to the Ru1-C1 in cyclometalated **6a** [1.948(3) Å]. This lengthening may be a consequence of a steric clash between the NHC ligand and more specifically of the mesityl group of the latter with the bulky *o*-(isopropoxy)benzylidene ligand located just below it.

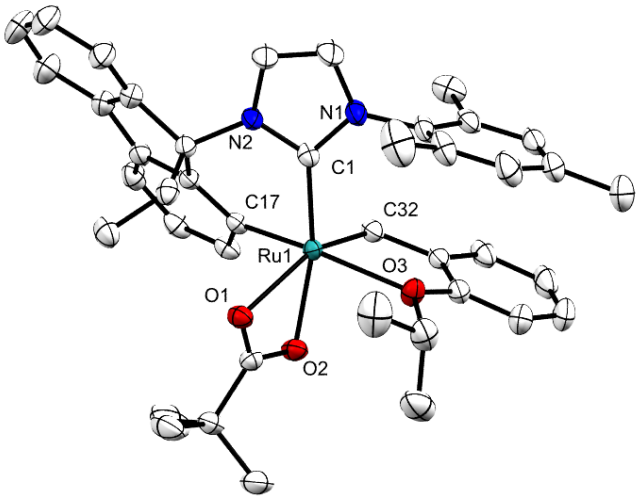

Figure 6. Molecular structure of **7b**. Ellipsoids drawn at the 30% probability level. Hydrogen atoms and solvent molecules were omitted for clarity. Selected bond distances (Å) and angles (deg): Ru1-C1 2.0767(18), Ru1-C32 1.8482(18), Ru1-C17 2.0003(17), Ru1-01 2.3528(12), Ru1-O2 2.1437(12), Ru1-O3 2.3820(13), C1-Ru1-C32 96.14(7), C1-Ru1-C17 85.99(7), C17-Ru1-C32 92.07(8).

The room temperature ^{1}H NMR spectrum of complex **7b** displayed many broad signals, which suggested a fluxional process in solution. A variable-temperature NMR experiment was therefore carried out. When the temperature was lowered to -50°C, all signals became sharper (Figure S9), indicating that the dynamic process was frozen at that temperature. The VT NMR behavior of complex **7b** is illustrated in Figure 7 on the benzylidene protons. While two very broad signals could be identified at δ = 17.36 and 16.11 ppm at 25°C indicating that two complexes are in rapid equilibrium, the exchange was stopped at – 50°C and two sharp singlets at δ = 17.32 and 16.10 ppm were observed in a 3:1 ratio. We tentatively assigned the major isomer as the "*cis*" complex observed in solid state and the minor isomer as the "*trans*" complex, in which the ether function of the o-(isopropoxy)benzylidene ligand is in *trans* position relative to the NHC.

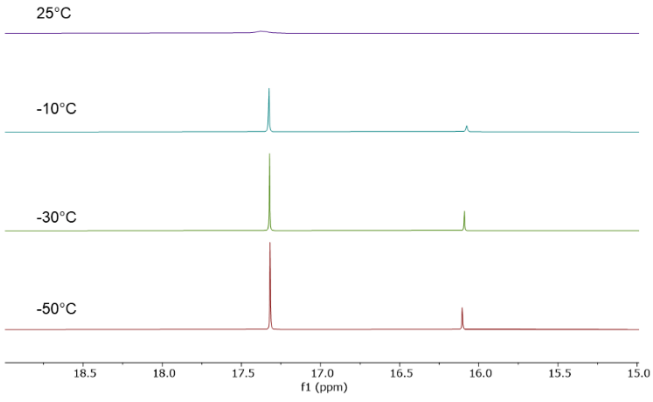

Figure 7. Variable temperature ^{1}H NMR spectra of complex **7b** in the region 19.0-15.0 ppm (THF-d_8, 600 MHz).

Catalytic activity of cyclometalated catalyst 6a

Our investigation on the catalytic activity of complex **6a** started by the ring closing metathesis (RCM) of diethyl diallylmalonate and of *N,N*-diallyl tosylamide using 1 mol% of **6a** in CH_2Cl_2 at room temperature. Unfortunately, no conversion could be detected under these conditions, neither by changing the solvent for THF and performing the reaction at 60°C. This lack of activity in RCM is in line with previous works reporting that the *Z*-selective carboxylate cyclometalated catalysts are not good catalysts in RCM.[6a]

We then turned our attention to the cross metathesis (CM) of allylbenzene (**8a**) with cis-1,2-diacetoxy-2-butene (**9**) using 2 mol% of **6a** in THF at 35°C (Scheme 4).[6b, 19] Due to the sensitivity of complex **6a** to oxygen, all manipulations were performed in a glove box. Furthermore, since ethylene can have a destructive effect on both reaction yield and selectivity,[20] the experiments were carried out in a vial open to the argon atmosphere inside the glove box. Gratifyingly, the conversion for the CM reaction of **8a** with **9** reached 58% after 1 h (c = 1M), and more importantly the alkene product **10a** was obtained in a high *Z/E* ratio (93/7). No homocoupling product **11a** was detected. However, neither the conversion nor the selectivity changed with a longer reaction time, suggesting that catalyst **6a** is rapidly deactivated during catalysis. The CM reaction was then performed at a higher concentration of 2 M and led to a conversion of 70% after 1 hour and to about the same Z/E selectivity (94/6) as in the previous experiment. Here again, no further evolution was detected after 1 h. The effect of reduced electron density of the alkene substrate was then examined by using 1-allyl-4-fluorobenzene (**8b**). While the conversion was noticeably reduced to 60%, the selectivity was not affected and remained at high levels.

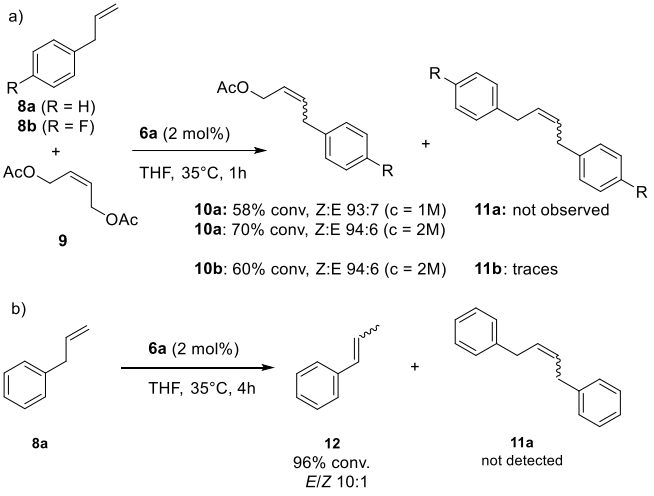

Scheme 4. a) Cross-metathesis of allylarenes **8a-b** with *cis*-1,4-diacetoxy-2-butene **9** catalyzed by **6a**. b) Isomerization of allylbenzene **8a** upon treatment with **6a**. Conversions were determined by GC analysis against a calibrated internal standard (tetradecane).

Eventually, we decided to study the homodimerization of allylbenzene, under the same reaction conditions. Unfortunately, the only product observed was 1-phenylpropene **12**, which resulted from isomerization of the double bond. These results were in agreement with the decomposition of complex **6a** into the Ru-H complex **6a'**, which is able to isomerize double bonds.[21]

The reaction of complex **6a** with an atmosphere of ethylene was also carried out to study the fate of complex under catalytic conditions. In an NMR tube, ethylene gas was bubbled into a solution of complex **6a** in benzene at room temperature, which induced a rapid color change of the solution from deep blue to yellow. (Scheme 5). The complex **13a** was generated in quantitative yield after 5 min at room temperature and its molecular structure was inferred from ^{1}H and ^{13}C NMR spectroscopy supplemented by 2D NMR experiments. Complex **13a** exhibited the same coordinated alkene moiety as complex **6a'**, which was characterized by a set of two doublets in ^{1}H NMR at δ = 4.71 and 4.51 ppm with a coupling constant of 8.1 Hz and by the corresponding ^{13}C resonances at δ = 64.6 and 40.7 ppm.[17] More importantly, the Ru-Et moiety could also be assessed by the two signals of the diastereotopic CH_2 protons at δ = 3.38 ppm (qd, *J* = 6.9, 4.6 Hz) and 2.82 ppm (qd, *J* = 6.9, 4.6 Hz) associated with the triplet signal of the terminal CH_3 protons at δ = - 0.27 ppm (*J* = 6.9 Hz). The formation of complex **13a** could be explained by the formation *in situ* of complex **6a'**, followed by insertion of ethylene into the Ru-H bond of **6a'**.

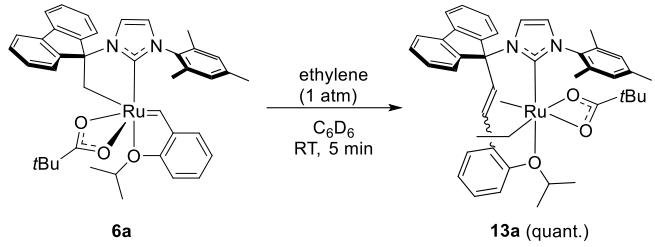

6a **13a** (quant.)

Scheme 5. Reaction of complex **6a** with ethylene gas.

Silver-mediated insertion of the benzylidene moiety into the Ru-NHC bond

As the benzyl-derivative **3c** did not react with NaOPiv most probably due to steric congestion, we devised to generate a cationic benzylidene complex by abstracting a chloride ligand, which would be more prone to react with NaOPiv in a subsequent cyclometallation reaction. Several cationic catalysts, in which the ruthenium center is positively charged, have been reported.[22] The abstraction of a chloride ligand in Ru-based alkylidene complexes is usually achieved by the use of a silver salt according to the first example described by Buchmeiser for the replacement of chloride ligand by another anionic ligand.[23] Hence, complexes **3a-c** were reacted with one equivalent of $AgSbF_6$ in CH_2Cl_2 at room temperature (Scheme 6). The reaction color turned rapidly from dark green to brick red and was accompanied by the disappearance of NMR benzylidene signal. After AgCl filtration and purification by precipitation, complexes **14a-c** were isolated in pure form in 46%, 43%, and 49% yield, respectively. They were characterized by ^{1}H and ^{13}C NMR spectroscopy, HRMS, and supplemented by single-crystal X-Ray diffraction on both complexes **14b** (Figure 8) and **14c** (Figure 9). Unexpectedly, they appeared to be 18e, piano-stool, Ru(II) complexes, supported by a new tridentate *ansa*-fluorenyl/N-heterocyclic olefin (NHO)/ether ligand, which originated from an unprecedented insertion of the benzylidene moiety into the Ru-NHC bond. The NHO ligand is a carbon-based donor composed of an alkylidene moiety appended to an NHC frame of general formula NHC=CR_2. Because of the highly polarized nature of the alkylidene in NHO, the zwitterionic imidazolium ylide form $(NHC)^{+}$-CR_2^{-} is predominant in coordination chemistry, where the NHO ligand acts as globally neutral 2σ-electron donor.[24] However, examples of well-defined metal-NHO complexes remain rather rare in literature,[25] and complexes **14a-c** thus constitute the first examples of NHO complexes, where the NHO ligand is generated in the coordination sphere by direct insertion of the alkylidene ligand into the Ru-NHC bond. The NHO ligands are characterized in ^{1}H NMR spectra by a singlet at δ = 4.60, 4.64, and 4.63 ppm in **14a-c**, respectively, accounting for the Ru-C*H* proton and by signals at δ = 34.8, 35.2, and 35.2 ppm in ^{13}C NMR spectra of **14a-c** corresponding to the ligated carbon atom.

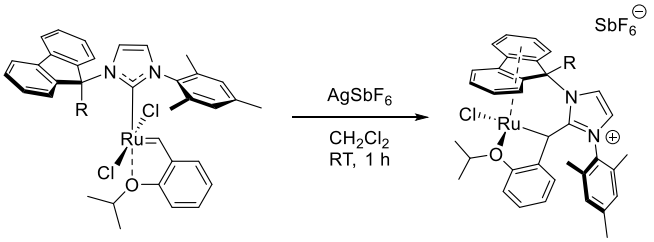

3a-c

14a (46%)
14b (46%)
14c (49%)

Scheme 6. Synthesis of the *ansa*-fluorenyl-NHO complexes **14a-c**.

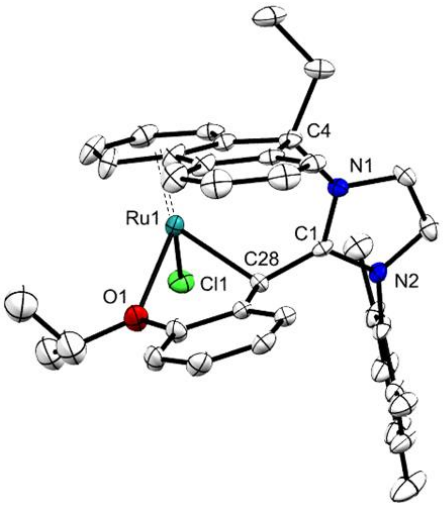

Figure 8. Molecular structure of **14b**. Ellipsoids drawn at the 30% probability level. Hydrogen atoms and solvent molecules were omitted for clarity. Selected bond distances (Å) and angles (deg): Ru1-C28 2.132(3), Ru1-Cl1 2.3954(9), Ru1-O1 2.240(3), C1-C28 1.462(5), C1-C28-Ru1 115.5(2).

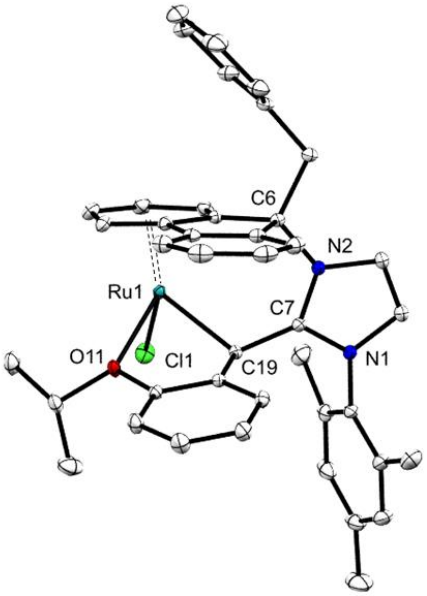

Figure 9. Molecular structure of **14c**. Ellipsoids drawn at the 30% probability level. Hydrogen atoms and solvent molecules were omitted for clarity. Selected bond distances (Å) and angles (deg): Ru1-C19 2.1341(9), Ru1-Cl1 2.4047(3), Ru1-O11 2.2133(7), C7-C19 1.4778(12), C7-C19-Ru1 116.48(6).

In order to gain more insight into this unusual migration reaction, DFT calculations were carried out on the transformation of the benzyl-derived complex **3c** into **14c** (Figure 10). First, the DFT calculations confirmed the conformation observed in neutral complex **3c**, in which the dangling benzyl group points towards the coordination sphere. Indeed, the other conformation **3c"**, obtained by a 180° rotation around the N-$C_{fluorenyl}$ bond is 9.6 kcal/mol higher in energy than the conformation **3c**, so experimentally the only observable conformation is the latter one. The abstraction of one chloride from **3c** led to the cationic complex **15c**, whose energy was set at 0 kcal/mol and all other Gibbs free energies were calculated relative to this one. In the optimized structure of **15c**, the Ru-alkylidene bond is in *cis* position to the NHC but is almost orthogonal to the carbenic heterocycle and there is an additional agostic C-H···Ru interaction stabilizing complex **15c**. Nevertheless, complex **15c** interconverts through rotation around the N-$C_{fluorenyl}$ bond into the much more stable conformer **15c"** in an almost barrierless reaction ($\Delta G^{\neq}$ = 3.2 kcal/mol). In complex **15c"**, a η^2-coordination of one C=C bond of the fluorenyl with the Ru center was identified. The insertion of the alkylidene occurs from this intermediate **15c"** with a barrier at 7.5 kcal/mol (24.1 kcal/mol with respect to **15c"**), consistent with experimental data showing a relatively fast formation of **14c** at room temperature. In **$TS_{15c\text{-}14c}$**, one aryl ring of the fluorenyl already coordinates the Ru center through a η^6 coordination mode. The Gibbs free energy of the final product **14c** is – 30.5 kcal/mol, in agreement with an irreversible reaction.

Conclusion

In order to design efficient *Z*-selective olefin metathesis catalysts based on the Grubbs' approach of cyclometalated chelating alkyl-NHC ligand, we developed the ligand family based on the N-(9-alkylfluoren-9-yl)imidazol-2-ylidene core and its coordination to Hoveyda-type ruthenium complexes. The cyclometalation reaction appeared to be highly dependent on the nature of the alkyl dangling group on the fluorenyl moiety, as only the methyl derivative **3a** gave the expected cyclometalated complex **6a**, while the ethyl derivative **3b** underwent a C(sp^2)-H activation of the fluorenyl part and the benzyl derivative was not reactive.
The cyclometalated complex **6a** was found to be highly sensitive towards air and moisture and also to slowly decompose by insertion of alkylidene into the Ru-alkyl bond. Although the catalytic activity of **6a** in the cross metathesis reaction is relatively low, the high *Z/E* ratio of 94/6 of the alkene product confirmed that this strategy of chelating cyclometalated (C,C_{NHC}) ligand is efficient in terms of stereoselectivity.
Finally, we reported an original, silver-induced, alkylidene insertion into the Ru-C_{NHC} bond to generate *ansa*-fluorenyl/N-heterocyclic olefins ligands.

Experimental Section

General Comments

All manipulations were carried out in dry glassware under nitrogen or argon atmosphere using standard vacuum line and Schlenk techniques, or in a glovebox under an argon atmosphere. N-mesitylimidazole,[26] 1-mesityl-3-(fluoren-9-yl) bromide,[10] and 1-mesityl-3-(fluorenid-9-yl) imidazolium[10] were synthesized according to literature procedures. All other reagents were commercially-available and used without further purification unless otherwise noted. Dry and oxygen-free organic solvents (THF, Et_2O, CH_2Cl_2, toluene) were obtained using LabSolv (Innovative Technology) or mBraun's SPS solvent purification systems. Hexane, pentane, and MeCN were used freshly distilled over calcium hydride under an atmosphere of argon. ^{1}H, ^{13}C, and ^{31}P NMR spectra were recorded on Agilent Mercury 400 MHz, Bruker Avance 400 MHz, Avance III HD 400 MHz, or Avance 300 MHz spectrometers. Chemical shifts (δ) are given in ppm and referred to residual solvent signals.[27] Coupling constants (*J*) are reported in hertz (Hz). Deuterated solvents as: CD_3OD, THF-d_8, CD_2Cl_2 and C_6D_6 were degassed by bubbling argon or freeze-pump-thaw method and dried over 3Å molecular sieves. Mass spectra (ESI mode) were obtained using a Xevo G2 QTof (Waters) spectrometer and were performed by the mass spectrometry service of the "Institut de chimie de Toulouse". High-resolution electrospray mass spectra (ESI-HRMS) were recorded on a Quattro LC triple quadrupole mass spectrometer. IR spectra were recorded on a Perkin-Elmer Spectrum 100 FT-IR spectrometer. The obtained data were processed with the software Omnic32. Wavenumbers are given in cm^{-1}. Elemental analyses were carried out by the elemental analysis service of the LCC (Toulouse, France) using a Perkin Elmer 2400 series II analyzer or in the Institute of Organic Chemistry Polish Academy of Sciences.

General procedure for the preparation of imidazolium tetrafluoroborates using KHMDS

1•HBr (1 equiv.) was dried in a Schlenk flask at 60 °C under high vacuum for 0.5 hour. After cooling down to room temperature, THF was added, and the suspension was cooled to –50 °C followed by dropwise addition of KHMDS (0.5 M in toluene, 1.02 equiv.). The bright yellow suspension was stirred at –50 °C for 1 h and allowed to warm to room temperature. All volatiles were removed under high vacuum and DMF was added. The solution of zwitterion **1** in DMF was cooled down to 0 °C followed by addition of the appropriate alkylating agent (RX, 2 equiv.). The reaction mixture was allowed to warm to room temperature and stirred overnight. Next, DMF was evaporated under high vacuum and the resulting solid was dissolved in CH_2Cl_2 and filtered through Celite to remove inorganic salts. The solution was concentrated to about 2 mL and 2 mL of H_2O were added immediately after adding $NaBF_4$ (2 equiv.).

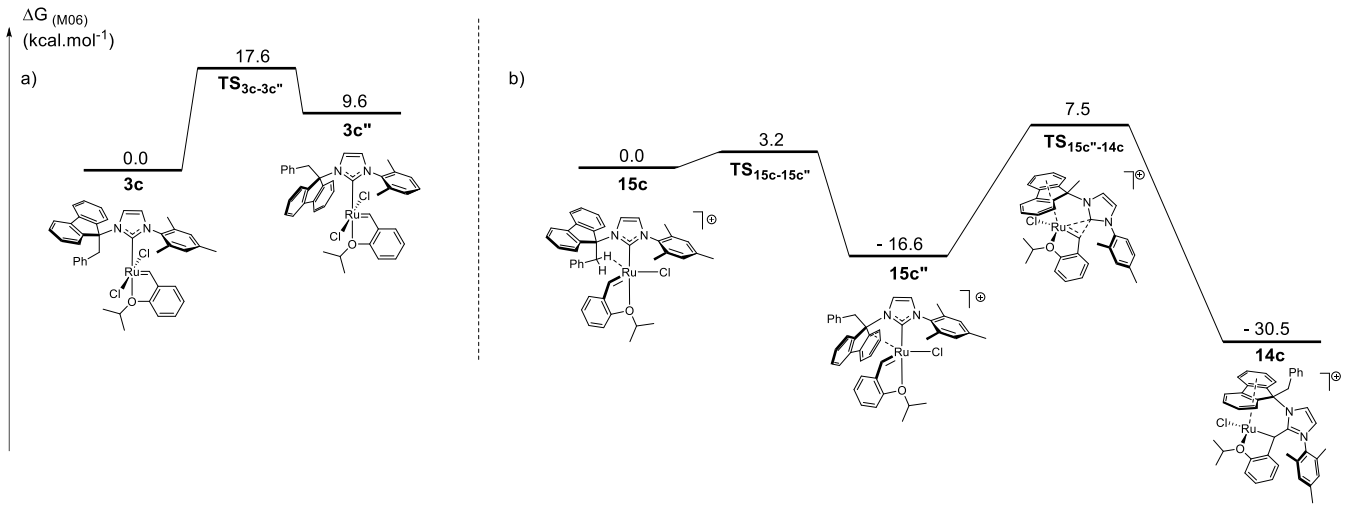

Figure 10. The free energy profile of a) the flip of the fluorenyl group in the neutral complexes **3c-3c"** and b) the transformation of the cationic complex **15c** into complex **14c**.

The mixture was stirred vigorously for 1 h for complete counterion metathesis. Phases were separated and the water layer was extracted with CH_2Cl_2. The organic phases were combined, dried over sodium sulfate, filtered and the solvent was then removed in vacuo. The crude product was purified using column chromatography (CombiFlash, silica gel, CH_2Cl_2/MeOH), precipitated from CH_2Cl_2/Et_2O, filtered, and washed with diethyl ether.

1-Mesityl-3-(9-methylfluoren-9-yl)imidazolium tetrafluoroborate (2a•HBF_4)

Following the general procedure, zwitterion **1** was obtained starting from **1**•HBr (1.39 mmol, 600 mg) and KHDMS (0.5 M in toluene, 1.42 mmol, 2.84 mL) in THF (15 mL). Next, iodomethane (2.78 mmol, 173 µL) and DMF (6 mL) were used for the alkylation step. Counterion exchange was achieved using $NaBF_4$ (2.78 mmol, 305 mg) in CH_2Cl_2/H_2O. Purification steps yielded **2a•**HBF_4 as a white solid (510 mg, 81%). ^{1}H NMR (400 MHz, $CDCl_3$) δ 9.11 (t, *J* = 1.7 Hz, 1H, N_2CH), 7.77 (dt, *J* = 7.6, 0.9 Hz, 2H, CH_{Flu}), 7.57 (dt, *J* = 7.6, 0.9 Hz, 2H, CH_{Flu}), 7.50 (td, *J* = 7.5, 1.1 Hz, 2H, CH_{Flu}), 7.39 (td, *J* = 7.5, 1.1 Hz, 2H, CH_{Flu}), 7.14 (t, *J* = 1.8 Hz, 1H, CH_{Im}), 7.05 (t, *J* = 1.9 Hz, 1H, CH_{Im}), 6.95 (d, *J* = 1.2 Hz, 2H, CH_{Mes}), 2.32 (s, 3H, $CH_{3\ Flu}$), 2.28 (s, 3H, $CH_{3\ Mes}$), 2.02 (s, 6H, $CH_{3\ Mes}$). ^{13}C{^{1}H} NMR (101 MHz, $CDCl_3$) δ 145.0 (C_{Flu}), 141.3 (C_{Mes}), 139.2 (C_{Flu}), 135.7 (N_2CH), 134.4 (C_{Mes}), 130.84 (CH_{Flu}), 130.81 (C_{Mes}), 129.9 (CH_{Mes}), 129.6 (CH_{Flu}), 124.5 (CH_{Im}), 123.8 (CH_{Flu}), 121.6 (CH_{Im}), 121.1 (CH_{Flu}), 71.1 ($C_{Flu\text{-}9}$), 23.5(CH_3), 21.2 ($CH_{3\ para}$), 17.3 ($CH_{3\ ortho}$). Elemental analysis calcd (%) for $C_{26}H_{25}BF_4N_2$ (Mw = 452.30): C 69.04, H 5.57, N 6.19; found: C 68.77, H 5.51, N 6.13.

1-Mesityl-3-(9-ethylfluoren-9-yl)imidazolium tetrafluoroborate (2b•HBF_4)

Following the general procedure, zwitterion **1** was obtained starting from **1**•HBr (2.32 mmol, 1 g) and KHDMS (0.5 M in toluene, 2.36 mmol, 4.7 mL) in THF (25 mL). Next, bromoethane (4.64 mmol, 345 mL) and DMF (12 mL) were used for the alkylation step. Counterion exchange was achieved using $NaBF_4$ (4.64 mmol, 509 mg) in CH_2Cl_2/H_2O. Purification steps yielded **2b•**HBF_4 as a white solid (835 mg, 77 %). ^{1}H NMR (300 MHz, $CDCl_3$) δ 9.12 (s, 1H, N_2CH), 7.78 (d, *J* = 7.6 Hz, 2H, CH_{Flu}), 7.56-7.48 (m, 4H, CH_{Flu}), 7.42 (t, *J* = 7.5 Hz, 2H, CH_{Flu}), 7.19 (t, *J* = 1.8 Hz, 1H, CH_{Im}), 7.13 (t, *J* = 1.5 Hz, 1H, CH_{Im}), 7.00 (s, 2H, CH_{Mes}), 2.98 (q, *J* = 7.2 Hz, 2H, CH_2CH_3), 2.32 (s, 3H, $CH_{3\ Mes}$), 2.03 (s, 6H, $CH_{3\ Mes}$), 0.53 (t, *J* = 7.2 Hz, 2H, CH_2CH_3). ^{13}C{^{1}H} NMR (101 MHz, $CDCl_3$) δ 143.1 (C_{Flu}), 141.5 (C_{Mes}), 140.4 (C_{Flu}), 135.8 (N_2CH), 134.3 (C_{Mes}), 130.9 (CH_{Flu}), 130.8 (C_{Mes}),, 130.0 (CH_{Mes}), 129.6 (CH_{Flu}), 124.1 (CH_{Im}), 123.9 (CH_{Flu}), 121.8 (CH_{Im}), 121.1 (CH_{Flu}), 75.3 ($C_{Flu\text{-}9}$), 29.2 (CH_2CH_3) , 21.3 ($CH_{3\ para}$), 17.4 ($CH_{3\ ortho}$), 7.9 (CH_2CH_3). HRMS (ESI): *m/z* calcd. for $[C_{27}H_{27}N_2]^+$ 379.2169, found 379.2174; ε_r = 1.3 ppm. Elemental analysis calcd (%) for $C_{27}H_{27}BF_4N_2$ (M_w = 466.33): C 69.54, H 5.84, N 6.01; found: C 69.32, H 5.68, N 5.97.

1-Mesityl-3-(9-benzylfluoren-9-yl)imidazolium tetrafluoroborate (2c•HBF_4)

Following the general procedure, zwitterion **1** was obtained starting from **1**•HBr (1.39 mmol, 600 mg) and KHDMS (0.5 M in toluene, 1.42 mmol, 2.84 mL) in THF (15 mL). Next, benzyl bromide (2.78 mmol, 0.33 mL) and DMF (6 mL) were used for the alkylation step. Counterion exchange was achieved using $NaBF_4$ (2.78 mmol, 305 mg) in CH_2Cl_2/H_2O. Purification steps yielded **2c•**HBF_4 as a white solid (560 mg, 76%). ^{1}H NMR (400 MHz, $CDCl_3$) δ 9.05 (t, *J* = 1.6 Hz, 1H, N_2CH), 7.81 – 7.73 (m, 2H, CH_{Flu}), 7.54 – 7.47 (m, 2H, CH_{Flu}), 7.46 (t, *J* = 1.8 Hz, 1H, CH_{Im}), 7.45 – 7.38 (m, 4H, CH_{Flu}), 7.13 (t, *J* = 1.8 Hz, 1H, CH_{Im}), 6.94 (s, 2H, CH_{Mes}), 6.91 (t, *J* = 7.4 Hz, 1H, CH_{Ph}), 6.80 (t, *J* = 7.6 Hz, 2H, CH_{Ph}), 6.61 (d, *J* = 7.2 Hz, 2H, CH_{Ph}), 4.21 (s, 2H, CH_2), 2.29 (s, 3H, $CH_{3\ para}$), 2.02 (s, 6H, $CH_{3\ ortho}$). ^{13}C{^{1}H} NMR (101 MHz, $CDCl_3$) δ 142.6 (C_{Flu}), 141.4 (C_{Mes}), 140.3 (C_{Flu}), 135.5 (N_2CH), 134.4 (C_{Mes}), 132.4 (C_{Ar}), 130.8 (C_{Mes}), 130.74 (CH_{Ar}), 130.73 (CH_{Ar}), 129.9 (CH_{Mes}), 129.1 (CH_{Flu}), 127.5 (CH_{Ph}), 126.9 (CH_{Ph}), 125.0 (CH_{Flu}), 124.3 (CH_{Im}), 122.2 (CH_{Im}), 120.8 (CH_{Flu}), 75.1 ($C_{Flu\text{-}9}$), 41.8 (CH_2), 21.2 ($CH_{3\ para}$), 17.4 ($CH_{3\ ortho}$). HRMS (ESI): *m/z* calcd. for $[C_{32}H_{29}N_2]^+$ 441.2325, found 441.2326; ε_r = 0.2 ppm. Elemental analysis calcd (%) for $C_{32}H_{29}BF_4N_2$ (M_w = 528.40): C 72.74, H 5.53, N 5.30; found: C 72.62, H 5.56, N 5.26.

General procedure for the preparation of imidazolium tetrafluoroborates using K_2CO_3

To a stirred solution of imidazolium bromide **1**•HBr (1 equiv.) in dry CH_3CN, K_2CO_3 (2 equiv.) was added. The mixture was stirred for 30 minutes, in which the solution turns yellow along the reaction course. The alkylating agent (RX, 2 equiv.) was added and the reaction mixture was stirred overnight. The progress of the reaction was monitored by ^{1}H NMR or by TLC. Next, CH_3CN was evaporated under reduced pressure, CH_2Cl_2 was added, and the mixture was filtered to get rid of potassium carbonate. Imidazolium salt was purified by column chromatography (CH_2Cl_2/MeOH). After purification, to its solution in CH_2Cl_2 (2 mL) were added H_2O (2 mL) and $NaBF_4$ (2 equiv.). The mixture was vigorously stirred for 1 h. Phases were separated and the aqueous layer was extracted with CH_2Cl_2. Organic phases were combined and dried over sodium sulfate. After filtration, the imidazolium tetrafluoroborate salt was precipitated from CH_2Cl_2/Et_2O, filtered, and washed with diethyl ether.

1-Mesityl-3-(9-ethylfluoren-9-yl)imidazolium tetrafluoroborate (2b•HBF_4)

Following the general procedure, to a solution of **1**•HBr (1.16 mmol, 500 mg) and potassium carbonate (2.32 mmol, 324 mg) in dry acetonitrile (25 mL) bromoethane (2.32 mmol, 0.17 mL) was added. Counterion exchange was achieved using $NaBF_4$ (2.32 mmol, 255 mg). Precipitation from CH_2Cl_2/Et_2O yielded **2b**•HBF_4 as a white solid (420 mg, 78%).

1-Mesityl-3-(9-benzylfluoren-9-yl)imidazolium tetrafluoroborate (2c•HBF_4)

Following the general procedure, to a solution of **1**•HBr (2.32 mmol, 1 g) and potassium carbonate (4.64 mmol, 635 mg) in dry acetonitrile (50 mL) benzyl bromide (4.64 mmol, 0.56 mL) was added. Counterion exchange was achieved using $NaBF_4$ (4.64 mmol, 509 mg). Crystallization from CH_2Cl_2/Et_2O yielded **2c**•HBF_4 as a white solid (874 mg, 71%).

General procedure for the preparation of Hoveyda type pre-catalysts 3a-c

Imidazolium salt **2a-c**•HBF_4 (1.2 equiv.) was dried in a pre-heated Schlenk flask for 1 h under high vacuum. Dry and degassed hexane was then added under an inert gas atmosphere. To this vigorously stirred suspension, potassium *tert*-pentoxide (1.7 M in toluene, 1.2 equiv.) was added. During the course of the reaction, the solution became yellow. The solution was stirred until becoming clear and Hoveyda–Grubbs I generation complex (**Hov-I**, 1 equiv.) was added as a solid all at once. The Schlenk flask was placed in a pre-heated (65°C) oil bath. The progress of the reaction was monitored by TLC (hexane/ethyl acetate, 4:1). During the progress of the reaction, precipitation of a green solid was observed. After 30 minutes, the reaction mixture was cooled down to RT. The precipitate was filtrated and washed with pentane. Hoveyda-Grubbs type II generation complexes **3a-c** were purified by column chromatography (silica gel, 15% AcOEt/hexane) and precipitated from CH_2Cl_2/MeOH (1:3) using a rotary evaporator. The products were obtained as a green microcrystalline solid.

[1-(2,4,6-trimethylphenyl)-3-(9-methylfluoren-9-yl)imidazol-2-ylidene]dichloro(o-isopropoxyphenyl-methylene)ruthenium(II) (3a)

Following the general procedure, **2a**•HBF_4 (0.77 mmol, 350 mg) in dry hexane (16 mL) was treated with potassium *tert*-pentoxide (1.7 M in toluene, 0.77 mmol, 0.45 mL) to generate the carbene. Next, **Hov-I** (0.645 mmol, 387 mg) was added. Product was obtained as a green solid (287 mg, 65%). ^{1}H NMR (400 MHz, CD_2Cl_2) δ 17.05 (s, 1H, RuC*H*), 7.86 (dd, *J* = 15.1, 7.6 Hz, 4H, CH_{Flu}), 7.73-7.65 (m, 1H, CH_{Ar}), 7.49 (td, *J* = 7.5, 1.2 Hz, 2H, CH_{Flu}), 7.38 (td, *J* = 7.5, 1.1 Hz, 2H, CH_{Flu}), 7.17 (s, 2H, CH_{Mes}), 7.09-7.03 (m, 3H, CH_{Ar}), 6.71 (d, *J* = 2.2 Hz, 1H, CH_{Im}), 6.39 (d, *J* = 2.2 Hz, 1H, CH_{Im}), 5.14 (hept, *J* = 6.2 Hz, 1H, CH(CH_3)$_2$), 4.16 (s, 3H, C$H_{3\ Flu\text{-}9}$), 2.54 (s, 3H, C$H_{3\ para}$), 2.09 (s, 6H, C$H_{3\ ortho}$), 1.64 (d, *J* = 6.2 Hz, 6H, CH(CH_3)$_2$). ^{13}C{^{1}H} NMR (101 MHz, CD_2Cl_2) δ 307.6 (Ru*C*H), 172.6 (N_2C), 153.0 (C_{Ar}), 150.0 (C_{Flu}), 145.9 (C_{Ar}), 140.2 (C_{Mes}), 139.2 (C_{Flu}), 138.6, 137.9 (C_{Mes}), 130.7 (*C*H$_{Ar}$), 129.7, 129.6 (*C*H$_{Flu}$), 129.2 (*C*H$_{Mes}$), 125.7 (*C*H$_{Im}$), 125.3 (*C*H$_{Flu}$), 123.4 (*C*H$_{Ar}$), 123.2 (*C*H$_{Ar}$), 123.0 (*C*H$_{Im}$), 120.8 (*C*H$_{Flu}$), 113.7 (*C*H$_{Ar}$), 75.1 (*C*H(CH$_3$)$_2$, 70.7 ($C_{Flu\text{-}9}$) , 26.0 (*C*H$_{3\ Flu\text{-}9}$) , 22.5 (CH(*C*H$_3$)$_2$), 21.4 (*C*H$_{3\ para}$), 18.1 (*C*H$_{3\ ortho}$). MS-ESI (positive mode): *m/z* (%) = 1391 (94) [2M + Na]$^+$, 707 (100) [M + Na]$^+$, 649 (12) [M - Cl]$^+$, 365 (14) [imidazolium]$^+$. IR: 421, 522, 534, 573**,** 598, 684, 737, 748, 770, 841, 856, 929, 942, 989, 1037, 1056, 1097, 1111, 1155, 1206, 1270, 1298, 1331, 1379, 1397, 1447, 1475, 1576, 1590, 2006, 2162, 2919, 2985, 3130 cm^{-1}. Elemental analysis calcd (%) for $C_{36}H_{36}Cl_2N_2ORu$ (M_W = 684.67): C 63.15, H 5.30, Cl 10.36, N 4.09; found C 62.87, H 5.25, Cl 10.31, N 4.07.

[1-(2,4,6-trimethylphenyl)-3-(9-ethylfluoren-9-yl)imidazol-2-ylidene]dichloro(o-isopropoxyphenyl-methylene)ruthenium(II) (3b)

Following general procedure **2b**•HBF_4 (0.92 mmol, 429 mg) in dry hexane (20 mL) was treated with potassium *tert*-pentoxide (1.7 M in toluene, 0.92 mmol, 054 mL) to generate the carbene. Next, **Hov-I** (0.767 mmol, 460 mg) was added. Product was obtained as a green solid (408 mg, 76%). ^{1}H NMR (400 MHz, CD_2Cl_2) δ 17.08 (s, 1H, RuC*H*), 7.82 (dd, *J* = 7.7, 3.6 Hz, 4H, CH_{Flu}), 7.73-7.64 (m, 1H, CH_{Ar}), 7.49 (td, *J* = 7.5, 1.1 Hz, 2H, CH_{Flu}), 7.38 (td, *J* = 7.5, 1.1 Hz, 2H, CH_{Flu}), 7.16 (s, 2H, CH_{Mes}), 7.09-6.99 (m, 3H, CH_{Ar}), 6.68 (d, *J* = 2.2 Hz, 1H, CH_{Im}), 6.41 (d, *J* = 2.2 Hz, 1H, CH_{Im}), 5.31 (q, *J* = 7.0 Hz, 2H, CH_2CH$_3$), 5.15 (hept, *J* = 6.2 Hz, 1H, CH(CH_3)$_2$), 2.54 (s, 3H, C$H_{3\ para}$), 2.07 (s, 6H, C$H_{3\ ortho}$), 1.68 (d, *J* = 6.1 Hz, 6H, CH(CH_3)$_2$), 0.66 (t, *J* = 6.9 Hz, 3H, CH$_2$CH_3). ^{13}C{^{1}H} NMR (101 MHz, CD_2Cl_2) δ 307.2 (RuCH), 172.3 (N_2C), 152.9 (C_{Ar}), 148.1 (C_{Flu}), 146.2 (C_{Ar}), 140.8 (C_{Flu}), 140.3 (C_{Mes}), 138.8 (C_{Mes}), 138.0 (C_{Mes}), 130.8 (*C*H$_{Ar}$), 129.9 (*C*H$_{Flu}$), 129.7 (*C*H$_{Flu}$), 129.5 (*C*H$_{Mes}$), 125.5 (*C*H$_{Im}$), 125.4 (*C*H$_{Flu}$), 123.6 (*C*H$_{Ar}$), 123.5 (*C*H$_{Ar}$), 123.2 (*C*H$_{Im}$), 120.7 (*C*H$_{Flu}$), 113.9 (*C*H$_{Ar}$), 75.5 ($C_{Flu\text{-}9}$), 75.2 (*C*H(CH$_3$)$_2$), 30.2 (CH$_2$CH$_3$), 22.8 (CH(*C*H$_3$)$_2$), 21.6 (*C*H$_{3\ para}$), 18.3 (*C*H$_{3\ ortho}$), 8.4 (CH$_2$*C*H$_3$). MS-ESI (positive mode): *m/z* (%) = 1419 (13) [2M + Na]$^+$, 721 (100) [M + Na]$^+$, 663 (68) [M - Cl]$^+$, 379 (100) [imidazolium]$^+$. IR: 421, 438, 491, 522, 534, 571, 594, 651, 685, 735, 751, 766, 812, 838, 859, 878, 933, 1030, 1087, 1100, 1112, 1156, 1194, 1298, 1328, 1376, 1450, 1475, 1576, 1588, 2175, 2878, 2937, 2980, 3115 cm^{-1}. Elemental analysis calcd (%) for $C_{37}H_{38}Cl_2N_2ORu$ (M_W = 698.69): C 63.61, H 5.48, Cl 10.15, N 4.01; found C 63.67, H 5.43, Cl 10.16, N 4.13.

[1-(2,4,6-trimethylphenyl)-3-(9-benzylfluoren-9-yl)imidazol-2-ylidene]dichloro(*o*-isopropoxyphenyl-methylene)ruthenium(II) (3c)

Following general procedure **2c**•HBF_4 (0.379 mmol, 200 mg) in dry hexane (12 mL) was treated with potassium *tert*-pentoxide (1.7 M in toluene, 0.379 mmol, 0.22 mL.) to generate carbene. Next, **Hov-I** (0.315 mmol, 189 mg.) was added. Product **4c** was obtained as a green solid (173 mg, 72%). ^{1}H NMR (400 MHz, CD_2Cl_2) δ 17.08 (s, 1H, RuC*H*), 8.06-8.00 (m, 2H, CH_{Flu}), 7.67 (ddd, *J* = 8.4, 6.9, 2.3 Hz, 1H, CH_{Ar}), 7.54-7.48 (m, 2H, CH_{Flu}), 7.44-7.34 (m, 4H, CH_{Flu}), 7.19 (s, 2H, CH_{Mes}), 7.09-7.02 (m, 2H, CH_{Ar}), 7.00 (d, *J* = 8.5 Hz, 2H, CH_{Ar}), 6.96 (t, *J* = 7.4 Hz, 1H, CH_{Bn}), 6.85 (t, *J* = 7.6 Hz, 2H, CH_{Bn}), 6.75 (s, 2H, CH_2), 6.74 (d, *J* = 2.2 Hz, 1H, CH_{Im}), 6.68 (dd, *J* = 8.1, 1.0 Hz, 2H, CH_{Bn}), 6.44 (d, *J* = 2.2 Hz, 1H, CH_{Im}), 5.00 (hept, *J* = 6.6 Hz, 1H, CH(CH_3)$_2$), 2.55 (s, 3H, C$H_{3\ para}$), 2.13 (s, 6H, C$H_{3\ ortho}$), 1.36 (d, *J* = 6.2 Hz, 6H, CH(CH_3)$_2$). ^{13}C{^{1}H} NMR (101 MHz, CD_2Cl_2) δ 308.2, 307.8 (RuCH), 172.9 (N_2C), 153.1 (C_{Ar}), 147.8 (C_{Flu}), 146.1 (C_{Ar}), 140.6 (C_{Flu}), 140.4 (C_{Mes}), 138.8 (C_{Mes}), 138.0 (C_{Mes}), 134.4 (C_{Bn}), 131.7 (*C*H$_{Bn}$), 131.0 (*C*H$_{Ar}$), 129.8 (*C*H$_{Flu}$), 129.8 (*C*H$_{Mes}$), 129.0 (*C*H$_{Flu}$), 127.6 (*C*H$_{Bn}$), 126.8 (*C*H$_{Bn}$), 126.0 (*C*H$_{Flu}$), 125.6 (*C*H$_{Im}$), 123.6, 123.4, 123.3 (2*C*H$_{Flu}$ + *C*H$_{Im}$), 120.5 (*C*H$_{Flu}$), 113.9 (*C*H$_{Ar}$), 75.6 (*C*H(CH$_3$)$_2$), 75.5 ($C_{Flu\text{-}9}$), 42.7 (*C*H$_2$), 22.5 (CH(*C*H$_3$)$_2$), 21.6 (*C*H$_{3\ para}$), 18.37(*C*H$_{3\ ortho}$). MS-ESI (positive mode): *m/z* (%) = 1544 (47) [2M + Na]$^+$, 783 (100) [M + Na]$^+$, 725 (14) [M - Cl]$^+$. IR: 403, 421, 439, 572, 606, 634, 691, 705, 732, 750, 760, 781, 840, 901, 930, 1036, 1096, 1112, 1158, 1200, 1218, 1295, 1329, 1379, 1400, 1452, 1475, 1488, 1575, 1587, 1937, 1977, 2919, 2987, 3030, 3066, 3107 cm^{-1}. Elemental analysis calcd (%) for $C_{42}H_{40}Cl_2N_2ORu$ (M_W = 760.77): C 66.31, H 5.30, Cl 9.32, N 3.68; found C 66.11, H 5.26, Cl 9.20, N 3.63.

General procedure for the preparation of cyclometalated complexes

Cyclometalated complexes were synthesized using the procedure developed by Grubbs and co-workers.[28] In a glovebox, a Schlenk flask was charged with Hoveyda-type II generation catalyst **3a-b** (1 equiv.), NaOPiv (15 equiv.), and the mixture of THF/MeOH (1:1, 40 mL/mmol(Ru)). The Schlenk tube was capped and heated at 48 °C for 8 h. The progress of the reaction was monitored by ^{1}H NMR. The solvents were removed under high vacuum and the residue was dissolved in benzene or THF, filtered through the pad of celite, and concentrated to a deep green residue. The residue was recrystallized a few times (usually 3 times) from THF/pentane or benzene/heptane at -40°C. The resulting crystals were washed with pentane and dried under high vacuum.

Synthesis of 6a and 6a'

Following the general procedure, a Schlenk flask was charged with **3a** (0.295 mmol, 200 mg), THF-MeOH (1:1, 12 mL) and sodium pivalate (4.38 mmol, 544 mg) and the mixture was stirred for 8 h at 48 ℃. After evaporation of the solvent, the product **6a** was purified as a violet solid by

recrystallization from THF/pentane at –40 ℃ (87 mg, 42%), along with the side product **6a'** as a yellow solid (18 mg, 8%).

Complex 6a

^{1}H NMR (400 MHz, C_6D_6) δ 15.74 (s, 1H, RuC*H*), 7.81 (d, *J* = 7.3 Hz, 1H, C*H*$_{Flu}$), 7.56 (dd, *J* = 7.5, 1.6 Hz, 1H, C*H*$_{Ar}$), 7.52-7.46 (m, 2H, C*H*$_{Flu}$), 7.30-7.22 (m, 2H, 1 C*H*$_{Ar}$ + 1 C*H*$_{Flu}$), 7.18-7.03 (m, 3H, CH$_{Flu}$), 6.96-6.87 (m, 2H, 1 C*H*$_{Ar}$ + 1 C*H*$_{Flu}$), 6.79 (s, 1H, C*H*$_{Mes}$), 6.77p (s, 1H, C*H*$_{Mes}$), 6.58 (d, *J* = 8.3 Hz, 1H, C*H*$_{Ar}$), 5.97 (d, *J* = 2.2 Hz, 1H, C*H*$_{Im}$), 5.86 (d, *J* = 2.2 Hz, 1H, C*H*$_{Im}$), 4.51 (hept, *J* = 6.3 Hz, 1H, C*H*(CH$_3$)$_2$), 4.01 (d, *J* = 11.6 Hz, 1H, C*H*$_2$), 3.21 (d, *J* = 11.7 Hz, 1H, C*H*$_2$), 2.46 (s, 3H, C*H*$_{3\ para}$), 2.20 (s, 3H, C*H*$_{3\ ortho}$), 2.11 (s, 3H, C*H*$_{3\ ortho}$), 1.25 (s, 9H, C(C*H*$_3$)$_3$), 1.19 (d, *J* = 6.4 Hz, 3H, CH(C*H*$_3$)$_2$), 1.15 (d, *J* = 6.3 Hz, 3H, CH(C*H*$_3$)$_2$). ^{13}C{^{1}H} NMR (101 MHz, C_6D_6) δ 263.4 (RuCH), 188.5 (*C*O$_2$), 185.6 (N$_2$*C*), 155.6 (*C*$_{Ar}$), 153.4 (*C*$_{Flu}$), 151.0 (*C*$_{Flu}$), 144.2 (*C*$_{Ar}$), 139.6 (*C*$_{Ar}$), 138.9 (*C*$_{Ar}$), 137.5 (*C*$_{Mes}$), 137.2 (*C*$_{Mes}$), 136.7 (*C*$_{Mes}$), 135.7 (*C*$_{Mes}$), 129.4 (*C*H$_{Ar}$), 129.3 (*C*H$_{Mes}$), 129.1 (*C*H$_{Mes}$), 128.6 (*C*H$_{Flu}$), 128.2 (*C*H$_{Flu}$), 127.9 (*C*H$_{Flu}$), 126.1 (*C*H$_{Ar}$), 124.1 (*C*H$_{Flu}$), 123.4 (*C*H$_{Flu}$), 122.7 (*C*H$_{Ar}$), 122.6 (*C*H$_{Im}$), 122.1 (*C*H$_{Flu}$), 120.1 (*C*H$_{Flu}$), 119.9 (*C*H$_{Flu}$), 118.0 (*C*H$_{Im}$), 113.6 (*C*H$_{Ar}$), 77.5 (*C*$_{Flu\text{-}9}$), 75.3 (*C*H(CH$_3$)$_2$), 42.5 (*C*H$_2$), 39.8 (*C*(CH$_3$)$_3$), 28.3 (C(*C*H$_3$)$_3$), 21.8 (CH(*C*H$_3$)$_2$), 21.5 (CH(*C*H$_3$)$_3$), 21.0 (*C*H$_{3\ para}$), 18.8 (*C*H$_{3\ ortho}$), 18.4 (*C*H$_{3\ para}$). HRMS (ESI+): *m/z* calcd. for **[**$C_{41}H_{43}N_2O_3Ru]^+$ ([M-H]$^+$) 713.2317, found 713.2313. ε$_r$ = 0.5 ppm.

Complex 6a'

^{1}H NMR (400 MHz, CD_2Cl_2) δ 8.47 (d, *J* = 7.6 Hz, 1H, C*H*$_{Ar}$), 7.78-7.72 (m, 3H, C*H*$_{Ar}$), 7.48-7.43 (m, 3H, C*H*$_{Ar}$), 7.39-7.31 (m, 2H, C*H*$_{Ar}$), 6.97 (bs, 1H, C*H*$_{Mes}$), 6.95 (d, *J* = 8.4 Hz, 1H, C*H*$_{Ar}$), 6.91 (s, 1H, C*H*$_{Mes}$), 6.85 (dt, *J* = 7.4, 1.1 Hz, 1H, C*H*$_{Ar}$), 6.72 (d, *J* = 8.2 Hz, 1H, C*H*$_{Ar}$), 6.28 (d, *J* = 2.2 Hz 1H, C*H*$_{Im}$), 6.16 (d, *J* = 2.2 Hz, 1H, C*H*$_{Im}$), 4.39 (hept, *J* = 6.1 Hz, 1H, C*H*(CH$_3$)$_2$), 4.05 (d, *J* = 7.5 Hz, 1H, Ru(HC=C*H*)),), 3.31 (dd, *J* = 7.5, 2.4 Hz, 1H, Ru(HC=C*H*)),), 2.32 (s, 3H, C*H*$_{3\ Mes}$), 2.24 (s, 3H, C*H*$_{3\ Mes}$), 2.09 (s, 3H, C*H*$_{3\ Mes}$), 1.37 (d, *J* = 6.3 Hz, 3H, CH(C*H*$_3$)$_2$), 0.86 (d, *J* = 6.3 Hz, 3H, CH(C*H*$_3$)$_2$), 0.80 (s, 9H, C(C*H*$_3$)$_3$), -9.97 (s, 1H, Ru-*H*). ^{13}C NMR (101 MHz, CD_2Cl_2) δ 192.7 (*C*O$_2$), 186.2 (N$_2$*C*), 156.7, 149.8, 149.4, 140.9, 139.1, 138.2, 137.5, 137.0, 136.5, 136.2 (*C*$_{Ar}$), 129.3 (*C*H$_{Ar}$), 129.2 (*C*H$_{Mes}$), 129.2 (*C*H$_{Ar}$), 129.2 (*C*H$_{Ar}$), 128.6 (*C*H$_{Ar}$), 128.3 (*C*H$_{Mes}$), 127.8 (*C*H$_{Ar}$), 126.2 (*C*H$_{Ar}$)125.0 (*C*H$_{Ar}$), 124.6 (*C*H$_{Ar}$), 122.7 (*C*H$_{Ar}$), 122.0 (*C*H$_{Im}$), 120.4 (*C*H$_{Ar}$), 120.2 (*C*H$_{Ar}$), 117.4 (*C*H$_{Im}$), 116.1 (*C*H$_{Ar}$), 76.9 (*C*H(CH$_3$)$_2$), 75.5 (Ru(HC=*C*H)),), 64.6 (Ru(HC=*C*H)), 50.0 (*C*$_{Flu\text{-}9}$), 39.9 (*C*(CH$_3$)$_3$), 22.9 (C(*C*H$_3$)$_3$), 22.9 (CH(*C*H$_3$)$_2$), 21.2 (*C*H$_{3\ Mes}$), 20.3 (CH(*C*H$_3$)$_2$), 18.4 (*C*H$_{3\ Mes}$), 17.9 (*C*H$_{3\ Mes}$). MS-ESI (positive mode): *m/z* (%) = 645 (100) [M – OPiv + MeOH]$^+$.

Complex 7b

Following the general procedure, a Schlenk flask was purged with **3b** (0.251 mmol, 150 mg), THF-MeOH (1:1, 10 mL) and sodium pivalate (3.22 mmol, 400 mg) and the mixture was stirred for 8 h at 48 ℃. After evaporation of the solvent, the complex **7b** was obtained as the main product as green crystals (80 mg, 48%), along with a very small amount of violet crystals by recrystallization from THF/pentane in − 40℃. The molecular formula of the violet crystals could not firmly established. At 243K, the complex **7b** is composed of two isomers majo and mino in a ratio 3/1. For the description of the NMR spectra, the signals are assigned to the corresponding isomer (majo or mino). ^{1}H NMR (600 MHz, THF-d_8, 243 K) δ 17.32 (RuC*H*, majo), 16.09 ((RuC*H*, mino), 8.03 (d, *J* = 8.7 Hz, 1H, C*H*$_{Flu}$, mino), 7.97 (d, *J* = 7.3 Hz, 1H, C*H*$_{Flu}$, majo), 7.93 (d, *J* = 2.1 Hz, 1H, C*H*$_{Im}$, mino), 7.91 (d, *J* = 2.0 Hz, 1H, C*H*$_{Im}$, majo), 7.74 (d, *J* = 8.0 Hz, 1H, C*H*$_{Flu}$, majo), 7.70 (dd, *J* = 6.0, 2.7 Hz, 1H, C*H*$_{Flu}$, mino), 7.61 (t, *J* = 8.8 Hz, 1H, C*H*$_{Ar}$, mino), 7.50 (ddd, *J* = 8.6, 7.2, 1.7 Hz, 1H, C*H*$_{Ar}$, majo), 7.46-7.38 (m, 2H majo + 2H mino, C*H*$_{Flu}$), 7.32 (d, *J* = 5.6 Hz, 1H, C*H*$_{Ar}$, mino), 7.27 (dd, *J* = 7.5, 1.7 Hz, 1H, C*H*$_{Ar}$, majo), 7.21 (d, *J* = 5.6 Hz, 1H, C*H*$_{Ar}$, mino), 7.07-7.05 (m, 1H, C*H*$_{Flu}$, majo + 2H, C*H*$_{Im}$ + C*H*$_{Flu}$, mino), 6.98-6.95 (m, 2H, C*H*$_{Mes}$ + C*H*$_{Ar}$, mino), 6.94-6.92 (m, 2H, C*H*$_{Ar}$, majo), 6.95 (d, *J* = 7.5 Hz, C*H*$_{Flu}$, majo), 6.80 (s, 1H, C*H*$_{Mes}$, mino), 6.79 (d, *J* = 2.0 Hz, 1H, C*H*$_{Im}$, majo), 6.77 (d, *J* = 8.4 Hz, 1H, C*H*$_{Flu}$, majo), 6.67 (s, 1H, C*H*$_{Mes}$, majo), 6.51 (t, *J* = 7.4 Hz, 1H, C*H*$_{Flu}$, mino), 6.07 (d, *J* = 7.4 Hz, 1H, C*H*$_{Flu}$, mino), 5.87 (s, 1H, C*H*$_{Mes}$, majo), 5.29 (sept, *J* = 6.3 Hz, 1H, C*H*$_{iPr}$, mino), 4.84 (sept, *J* = 6.2 Hz, 1H, C*H*$_{iPr}$, majo), 4.04 (dq, *J* = 11.8, 7.1 Hz, 1H, C*H*$_{2\ Et}$, majo), 3.32 (dq, *J* = 14.4, 7.2 Hz, 1H, C*H*$_{2\ Et}$, mino), 3.04 (dq, *J* = 14.4, 7.2 Hz, 1H, C*H*$_{2\ Et}$, mino), 2.46 (dq, *J* = 11.7, 7.1 Hz, 1H, C*H*$_{2\ Et}$, majo), 2.34 (s, 3H, C*H*$_{3\ Mes}$, mino), 2.23 (s, 3H, C*H*$_{3\ Mes}$, mino), 2.03 (s, 3H, C*H*$_{3\ Mes}$, majo), 2.01 (s, 3H, C*H*$_{3\ Mes}$, majo), 1.97 (s, 3H, C*H*$_{3\ Mes}$, mino), 1.64 (d, *J* = 6.3 Hz, 3H, C*H*$_{3\ iPr}$, majo), 1.57 (d, *J* = 6.4 Hz, 3H, C*H*$_{3\ iPr}$, mino), 1.46 (d, *J* = 6.1 Hz, 3H, C*H*$_{3\ iPr}$, mino), 1.23 (d, *J* = 5.9 Hz, 3H, C*H*$_{3\ iPr}$, majo), 1.13 (s, 9H, C*H*$_{3\ tBu}$, mino), 1.03 (s, 3H, C*H*$_{3\ Mes}$, majo), 0.86 (s, 9H, C*H*$_{3\ tBu}$, majo), 0.63 (t, *J* = 7.2 Hz, 3H, C*H*$_{3\ Et}$, mino), 0.36 (t, *J* = 7.1 Hz, 3H, C*H*$_{3\ Et}$, majo). ^{13}C{^{1}H} NMR (151 MHz, THF-d_8, 243 K) δ 299.2 (RuCH, majo), 283.4 (RuCH, mino), 188.4 (*C*O$_2$, majo), 188.2 (*C*O$_2$, mino), 183.7 (N$_2$*C*, majo), 181.7 (N$_2$*C*, mino), 161.4 (*C*$_{Ar}$, majo), 156.2 (*C*$_{Ar}$, mino), 155.5 (*C*$_{Ar}$, majo), 154.4 (*C*$_{Ar}$, mino), 150.1 (*C*$_{Flu}$, majo), 150.0 (*C*$_{Flu}$, mino), 145.8 (*C*$_{Ar}$, mino), 145.7 (*C*$_{Flu}$, majo), 144.3 (Ru-*C*$_{Flu}$, majo), 144.3 (*C*$_{Ar}$, mino), 143.6 (*C*H$_{Flu}$, majo), 143.4 (Ru-*C*$_{Flu}$, mino), 138.5 (*C*$_{Mes}$, majo), 138.4, 138.2, 137.9 (*C*$_{Ar}$, mino), 136.3 (*C*$_{Mes}$, majo), 135.8 (*C*$_{Ar}$, mino), 135.7 (*C*H$_{Flu}$, mino), 135.7, 135.6 (*C*$_{Ar}$, mino), 134.7 (*C*$_{Mes}$, majo), 134.5 (*C*$_{Mes}$, majo), 129.5 (*C*H$_{Flu}$, majo), 129.2 (*C*H$_{Mes}$, mino), 128.6 (*C*H$_{Mes}$, mino), 128.2 (*C*H$_{Ar}$, mino), 128.0 (*C*H$_{Mes}$, majo), 129.9 (*C*H$_{Mes}$, majo), 127.5 (*C*H$_{Ar}$, majo), 126.8 (*C*H$_{Flu}$, mino), 126.75 (*C*H$_{Flu}$, mino), 126.5 (*C*H$_{Flu}$, majo), 126.45 (*C*H$_{Flu}$, majo), 125.6 (*C*H$_{Ar}$, majo), 124.4 (*C*H$_{Ar}$, mino), 124.1 (*C*H$_{Ar}$, mino), 124.0 (*C*H$_{Ar}$, majo), 123.5 (*C*H$_{Ar}$, mino), 123.3 (*C*H$_{Ar}$, mino), 122.3 (*C*H$_{Ar}$, majo), 122.2 (*C*H$_{Im}$, majo), 120.5 (*C*H$_{Im}$, mino), 120.4 (*C*H$_{Flu}$), 120.3 (*C*H$_{Im}$, majo), 120.1 (*C*H$_{Flu}$, mino), 114.9 (*C*H$_{Flu}$, majo), 113.9 (*C*H$_{Ar}$, mino), 112.1 (*C*H$_{Flu}$, majo), 77.0 (*C*$_{Flu\text{-}9}$, majo), 76.9 (*C*H$_{iPr}$, mino), 73.0 (*C*H$_{iPr}$, majo), 39.7 (*C*$_{tBu}$, mino), 39.1 (*C*$_{tBu}$, majo), 38.4 (*C*H$_{2\ Et}$, majo), 36.4 (*C*H$_{2\ Et}$, mino), 28.0 (*C*H$_{3\ tBu}$, mino), 27.6 (*C*H$_{3\ tBu}$, majo), 22.3 (*C*H$_{3\ iPr}$, majo), 21.8 (*C*H$_{3\ iPr}$, mino), 21.7 (*C*H$_{3\ iPr}$, mino), 21.05 (*C*H$_{3\ iPr}$, majo), 21.0 (*C*H$_{3\ Mes}$, mino), 20.7 (*C*H$_{3\ Mes}$, majo), 19.7 (*C*H$_{3\ Mes}$, mino), 19.05 (*C*H$_{3\ Mes}$, mino), 19.0 (*C*H$_{3\ Mes}$, majo), 17.8 (*C*H$_{3\ Mes}$, majo), 9.8 (*C*H$_{3\ Et}$, majo), 9.4 (*C*H$_{3\ Et}$, mino). HRMS (ESI): *m/z* calcd. for **[**$C_{42}H_{46}N_2O_3Ru]$ 728.2546, found 728.2552. ε$_r$ = 0.8 ppm.

Investigation into behaviour of catalyst 6a in the presence of ethylene – synthesis of 13a

In a glove box an NMR tube was charged with **6a** (0.07 mmol, 50 mg), dissolved in deuterated benzene (0.7 mL) and capped using rubber septum. Next, NMR tube was removed from the glovebox and the complex solution was purged with ethylene through a septum using a long needle. Within 5 minutes the solution changed colour from blue to yellow. After 10 minutes the ^{1}H NMR was measured. The NMR tube with the solution was placed in the glovebox. The solution was concentrated, layered with hexane and placed in a freezer (−40 ℃). ^{1}H NMR (400 MHz, C_6D_6) δ 9.00 (dt, *J* = 7.6, 1.0 Hz, 1H, C*H*$_{Flu}$), 8.09-8.04 (m, 1H, C*H*$_{Flu}$), 7.65-7.55 (m, 2H, C*H*$_{Flu}$), 7.52 (td, *J* = 7.5, 1.1 Hz, 1H, C*H*$_{Flu}$), 7.32 (td, *J* = 7.4, 1.1 Hz, 1H, C*H*$_{Flu}$), 7.21-7.11 (m, 2H, C*H*$_{Flu}$), 7.01 (dd, *J* = 7.9, 1.7 Hz, 1H, C*H*$_{Ar}$), 6.96 (ddd, *J* = 8.2, 7.3, 1.7 Hz, 1H, C*H*$_{Ar}$), 6.74 (td, *J* = 7.5, 1.1 Hz, 1H, C*H*$_{Ar}$), 6.67 (dd, *J* = 8.5, 1.3 Hz, 1H, C*H*$_{Ar}$), 6.65 (s, 1H, C*H*$_{Mes}$), 6.59 (s, 1H, C*H*$_{Mes}$), 5.95 (d, *J* = 2.2 Hz, 1H, C*H*$_{Im}$), 5.53 (d, *J* = 2.2 Hz, 1H, C*H*$_{Im}$), 4.71 (d, *J* = 8.1 Hz, 1H, Ru(HC=C*H*)), 4.51 (d, *J* = 8.2 Hz, 1H, Ru(HC=C*H*)), 4.45-4.43 (m, 1H, C*H*(CH$_3$)$_2$), 3.42-3.36 (m, 1H, C*H*$_{2\ Et}$), 2.82 (qd, *J* = 6.9, 4.5 Hz, 1H, C*H*$_{2\ Et}$), 2.26 (s, 3H, C*H*$_{3\ Mes}$), 2.03 (s, 3H, C*H*$_{3\ Mes}$), 1.98 (s, 3H, C*H*$_{3\ Mes}$), 1.28 (s, 9H, C(C*H*$_3$)$_3$), 1.27 (d, *J* = 6.0 Hz, 6H, CH(C*H*$_3$)$_2$), -0.27 (t, *J* = 6.9 Hz, 3H, C*H*$_{3\ Et}$). ^{13}C{^{1}H} NMR (101 MHz, C_6D_6) δ 193.5 (*C*O$_2$), 190.8 (N$_2$*C*), 155.1 (*C*$_{Ar}$), 150.7, 149.6, 141.5, 139.3 (*C*$_{Flu}$), 138.5 (*C*$_{Mes}$), 137.5 (*C*$_{Mes}$), 136.3 (*C*$_{Ar}$), 135.6 (*C*$_{Mes}$), 135.55 (*C*$_{Mes}$), 129.4 (*C*$_{Ar}$), 129.2 (*C*H$_{Mes}$), 129.1 (*C*H$_{Flu}$), 128.9 (*C*H$_{Mes}$), 128.8 (*C*H$_{Flu}$), 128.5 (*C*H$_{Ar}$), 128.2 (*C*H$_{Flu}$), 127.9 (*C*H$_{Flu}$), 127.2 (*C*H$_{Flu}$), 125.5 (*C*H$_{Flu}$), 124.8 (*C*H$_{Ar}$), 121.2 (*C*H$_{Im}$), 120.5 (*C*H$_{Ar}$), 120.2 (*C*H$_{Flu}$), 118.3 (*C*H$_{Im}$), 111.7 (*C*H$_{Ar}$), 76.3 (*C*$_{Flu\text{-}9}$), 68.4 (*C*H(CH$_3$)$_2$), 64.6 (Ru(HC=*C*H)), 40.7 (Ru(HC=*C*H)), 39.9 (*C*(CH$_3$)$_3$), 34.8 (CH$_{2\ Et}$), 27.7 (C(*C*H$_3$)$_3$), 22.6 (CH(*C*H$_3$)$_2$), 22.3 (CH(*C*H$_3$)$_2$), 21.0 (*C*H$_{3\ Mes}$), 18.5 (*C*H$_{3\ Mes}$), 17.8 (*C*H$_{3\ Mes}$), 4.1 (*C*H$_{3\ Et}$).

General procedure for the synthesis of complexes 14a-c

To a solution of Hoveyda second-generation catalyst **3a-c** (1 equiv.) in CH_2Cl_2 (~40-45 mL/mmol), silver hexafluoroantimonate(V) (1 equiv.) was added as a solid all at once. The reaction mixture was vigorously stirred for 1 hour. Within the first 30 minutes, the solution changed color from green to red. Further, the reaction mixture was filtered through a pad of celite and the final complex **14a-c** was purified by precipitation from CH_2Cl_2:MeOH on rotary evaporator.

Complex 14a

Following the general procedure **3a** (0.117 mmol, 80 mg), silver hexafluoroantimonate(V) (0.117 mmol, 40.1 mg) and CH_2Cl_2 (5 mL) were used. Product was obtained as a dark red solid (48 mg, 46%). ^{1}H NMR (400 MHz, CD_2Cl_2) δ 8.18 (d, *J* = 2.7 Hz, 1H, C*H*$_{Im}$), 7.47 (d, *J* = 7.7 Hz, 1H, C*H*$_{Flu}$), 7.37 (d, *J* = 2.4 Hz, 1H, C*H*$_{Im}$), 7.23 (ddd, *J* = 7.7, 6.6, 2.0 Hz, 1H, C*H*$_{Ar}$), 7.03-6.97 (m, 2H, C*H*$_{Ar}$), 6.96 (s, 1H, C*H*$_{Mes}$), 6.90 (s, 1H, C*H*$_{Mes}$), 6.68-6.61 (m, 1H, C*H*$_{Ar}$), 6.55 (d, *J* = 7.1 Hz, 1H, C*H*$_{Ar}$), 6.39 (t, *J* = 5.7 Hz, 1H, C*H*$_{Flu\ coord}$), 6.24 (td, *J* = 7.0, 1.2 Hz, 1H, C*H*$_{Ar}$), 6.18 (d, *J* = 6.1 Hz, 1H, C*H*$_{Flu\ coord}$), 5.91 (t, *J* = 6.0 Hz, 1H, C*H*$_{Flu\ coord}$), 5.75 (dt, *J* = 7.5, 1.5 Hz, 1H, C*H*$_{Ar}$), 4.82 (hept, *J* = 6.4 Hz, 1H, C*H*$(CH_3)_2$), 4.60 (s, 1H, Ru-C*H*), 4.12 (d, *J* = 5.6 Hz, 1H, C*H*$_{Flu\ coord}$), 2.39 (s, 3H, Flu-C*H*$_3$), 2.26 (s, 3H, C*H*$_{3\ Mes}$), 2.14 (s, 3H, C*H*$_{3\ Mes}$), 1.89 (s, 3H, C*H*$_{3\ Mes}$), 1.79 (d, *J* = 6.3 Hz, 3H, CH(C*H*$_3)_2$), 1.10 (d, *J* = 6.3 Hz, 3H, CH(C*H*$_3)_2$). ^{13}C{^{1}H} NMR (101 MHz, CD_2Cl_2) δ 156.6 (N_2*C*), 155.6 (*C*$_{Ar}$), 144.0 (*C*$_{Flu}$), 141.5 (*C*$_{Mes}$), 137.2 (*C*$_{Mes}$), 134.6 (*C*$_{Ar}$), 134.5 (*C*$_{Mes}$), 131.0 (*C*$_{Mes}$), 131.0 (*C*H$_{Ar}$), 130.1 (*C*H$_{Mes}$), 130.0 (*C*H$_{Ar}$), 129.9 (*C*H$_{Mes}$), 126.8 (*C*H$_{Ar}$), 126.5 (*C*H$_{Ar}$), 124.1 (*C*H$_{Ar}$), 122.9 (*C*H$_{Im}$), 122.6 (*C*H$_{Ar}$), 121.0 (*C*H$_{Im}$), 114.4 (*C*H$_{Ar}$), 111.4 (*C*$_{Flu}$), 92.4 (*C*H$_{Flu}$), 89.7 (*C*$_{Flu}$), 86.8 (*C*H$_{Flu}$), 83.2 (*C*H$_{Flu}$), 79.3 (*C*H$(CH_3)_2$), 68.7 (*C*$_{Flu\text{-}9}$), 51.4 (*C*H$_{Flu}$), 34.8 (Ru-*C*H), 27.9 (Flu-*C*H$_3$), 23.1 (CH(*C*H$_3)_2$), 21.7 (CH(*C*H$_3)_2$), 21.1 (C*H*$_{3\ Mes}$), 18.5 (C*H*$_{3\ Mes}$), 18.1 (C*H*$_{3\ Mes}$). HRMS (ESI): *m/z* calcd. for **[**$C_{36}H_{36}ClN_2ORu]^+$ ([M – $SbF_6]^+$) 649.1554, found 649.1564; ε_r = 1.5 ppm.

Complex 14b

Following the general procedure **3b** (0.143 mmol, 100 mg), silver hexafluoroantimonate(V) (0.143 mmol, 49.2 mg) and CH_2Cl_2 (6 mL) were used. Product was obtained as a dark red solid (60 mg, 46 %). ^{1}H NMR (400 MHz, CD_2Cl_2) δ 8.23 (d, *J* = 2.4 Hz, 1H, C*H*$_{Im}$), 7.42 (dt, *J* = 7.7, 0.9 Hz, 1H, C*H*$_{Flu}$), 7.38 (d, *J* = 2.4 Hz, 1H, C*H*$_{Im}$), 7.25 (td, *J* = 7.6, 1.2 Hz, 1H, C*H*$_{Flu}$), 7.00 (td, *J* = 7.5, 1.0 Hz, 1H, C*H*$_{Flu}$), 6.96 (brs, 1H, C*H*$_{Mes}$), 6.93 (ddd, *J* = 7.8, 1.2, 0.7 Hz, 1H, C*H*$_{Flu}$), 6.90 (brs, 1H, C*H*$_{Mes}$), 6.69-6.60 (m, 1H, C*H*$_{Ar}$), 6.55 (d, *J* = 7.3 Hz, 1H, C*H*$_{Ar}$), 6.41 (td, *J* = 5.9, 0.5 Hz, 1H, C*H*$_{Flu}$), 6.24 (td, *J* = 7.5, 0.6 Hz, 1H, C*H*$_{Ar}$), 6.14 (dt, *J* = 6.0, 0.7 Hz, 1H, C*H*$_{Flu}$), 5.92 (td, *J* = 5.7, 0.6 Hz, 1H, C*H*$_{Flu}$), 5.74 (dt, *J* = 7.5, 1.4 Hz, 1H, C*H*$_{Ar}$), 4.81 (hept, *J* = 6.3 Hz, 1H, C*H*$(CH_3)_2$), 4.64 (s, 1H, RuC*H*), 4.03 (d, *J* = 5.6 Hz, 1H, C*H*$_{Flu}$), 3.12-2.98 (m, 1H, C*H*$_2$CH$_3$), 2.83-2.68 (m, 1H, C*H*$_2$CH$_3$), 2.26 (s, 3H, C*H*$_{3\ para}$), 2.14 (s, 3H, C*H*$_{3\ ortho}$), 1.88 (s, 3H, C*H*$_{3\ ortho}$), 1.79 (d, *J* = 6.3 Hz, 3H, CH(C*H*$_3)_2$), 1.10 (d, *J* = 6.2 Hz, 3H, CH$_2$(C*H*$_3)_2$), 0.62 (t, *J* = 7.3 Hz, 3H, CH$_2$C*H*$_3$). ^{13}C{^{1}H} NMR (101 MHz, CD_2Cl_2) δ 156.9 (N_2*C*), 155.8 (*C*$_{Ar}$), 142.4 (*C*$_{Flu}$), 141.7 (*C*$_{Mes}$), 137.3 (*C*$_{Mes}$), 136.0 (*C*$_{Flu}$), 134.9 (*C*$_{Ar}$), 134.7 (*C*$_{Mes}$), 131.3 (*C*H$_{Flu}$), 131.3 (*C*$_{Mes}$), 130.3 (*C*H$_{Mes}$), 130.1 (*C*H$_{Flu}$), 126.9 (*C*H$_{Ar}$), 126.7 (*C*H$_{Ar}$), 124.1 (*C*H$_{Flu}$), 123.2 (*C*H$_{Im}$), 122.8 (*C*H$_{Ar}$), 122.4 (*C*H$_{Flu}$), 120.7 (*C*H$_{Im}$), 114.6 (*C*H$_{Ar}$), 110.1 (*C*$_{Flu}$), 92.7 (*C*H$_{Flu}$), 90.7 (*C*$_{Flu}$), 87.1 (*C*H$_{Flu}$), 83.0 (*C*H$_{Flu}$), 79.5 (*C*H$(CH_3)_2$), 72.7 (*C*$_{Flu\text{-}9}$) , 51.3 (*C*H$_{Flu}$), 35.2 (RuCH), 33.1 (*C*H$_2$CH$_3$), 23.2 (CH(*C*H$_3)_2$), 21.8 (CH(*C*H$_3)_2$), 21.3 (C*H*$_{3\ para}$), 18.7 (C*H*$_{3\ ortho}$), 18.3 (C*H*$_{3\ ortho}$), 8.10 (CH$_2$*C*H$_3$). HRMS (ESI): *m/z* calcd. for $[C_{37}H_{38}ClN_2ORu]^+$ ([M – $SbF_6]^+$) 663.1711, found 663.1729; ε_r = 2.7 ppm.

Complex 14c

Following the general procedure, **3c** (0.206 mmol, 157 mg), silver hexafluoroantimonate(V) (0.206 mmol, 70.9 mg) and CH_2Cl_2 (8 mL) where used. Product was obtained as a dark red solid (98 mg, 49%). ^{1}H NMR (400 MHz, CD_2Cl_2) δ 8.40 (d, *J* = 2.4 Hz, 1H, C*H*$_{Im}$), 7.68-7.61 (d, *J* = 7.7 Hz, 1H, C*H*$_{Flu}$), 7.44 (d, *J* = 2.4 Hz, 1H, C*H*$_{Im}$), 7.29 (td, *J* = 7.7, 0.9 Hz, 1H, C*H*$_{Flu}$), 7.02-6.96 (m, 2H, C*H*$_{Bn}$ + C*H*$_{Mes}$), 6.94 (dd, *J* = 7.7, 0.9 Hz, 1H, C*H*$_{Flu}$), 6.92 (br s, 1H, C*H*$_{Mes}$), 6.84 (t, *J* = 7.7 Hz, 2H, C*H*$_{Bn}$), 6.66 (d, *J* = 7.7 Hz, 1H, C*H*$_{Flu}$), 6.65-6.58 (m, 1H, C*H*$_{Ar}$), 6.50-6.45 (m, 3H, 2 C*H*$_{Bn}$ + C*H*$_{Ar}$), 6.31-6.22 (m, 2H, C*H*$_{Flu\ coord.}$ + C*H*$_{Ar}$), 5.88 (t, *J* = 5.6 Hz, 1H, C*H*$_{Flu\ coord.}$), 5.83-5.79 (m, 2H, C*H*$_{Ar}$ + C*H*$_{Flu\ coord.}$), 4.76 (hept, *J* = 6.3 Hz, 1H, C*H*$(CH_3)_2$), 4.63 (s, 1H, Ru-C*H*), 4.42 (d, *J* = 11.8 Hz, 1H, C*H*$_2$), 4.26 (d, *J* = 5.5 Hz, 1H, C*H*$_{Flu\ coord}$), 4.01 (d, *J* = 11.8 Hz, 1H, C*H*$_2$), 2.27 (s, 3H, C*H*$_{3\ Mes}$), 2.19 (s, 3H, C*H*$_{3\ Mes}$), 1.93 (s, 3H, C*H*$_{3\ Mes}$), 1.73 (d, *J* = 6.3 Hz, 3H, CH(C*H*$_3)_2$), 1.07 (d, *J* = 6.3 Hz, 3H, CH(C*H*$_3)_2$). ^{13}C{^{1}H} NMR (101 MHz, CD_2Cl_2) δ 157.1 (N_2*C*), 155.5 (*C*$_{Ar}$), 142.2 (*C*$_{Flu}$), 141.7 (*C*$_{Mes}$), 137.4 (*C*$_{Mes}$), 136.2 (*C*$_{Flu}$), 134.7 (*C*$_{Mes}$), 134.7 (*C*$_{Ar}$) 131.3 (*C*H$_{Bn}$), 131.3 (*C*$_{Mes}$), 131.2 (*C*$_{Bn}$), 130.3 (*C*H$_{Mes}$), 130.1 (*C*H$_{Flu}$), 130.0 (*C*H$_{Mes}$), 128.2 (*C*H$_{Bn}$), 128.1 (*C*H$_{Flu}$), 127.0 (*C*H$_{Ar}$), 126.9 (*C*H$_{Ar}$), 125.1 (*C*H$_{Flu}$), 123.3 (*C*H$_{Im}$), 122.8 (*C*H$_{Ar}$), 122.1 (*C*H$_{Flu}$), 120.8 (*C*H$_{Im}$), 114.5 (*C*H$_{Ar}$), 109.9 (*C*$_{Flu}$), 92.0 (*C*H$_{Flu}$), 90.0 (*C*$_{Flu}$), 86.9 (*C*H$_{Flu}$), 83.0 (*C*H$_{Flu}$), 79.5 (*C*H$(CH_3)_2$), 72.4 (*C*$_{Flu\text{-}9}$), 52.1 (*C*H$_{Flu}$), 45.6 (*C*H$_2$), 35.2 (Ru-*C*H), 23.2 (CH(*C*H$_3)_2$), 21.8 (CH(*C*H$_3)_2$), 21.3 (C*H*$_{3\ Mes}$), 18.8 (C*H*$_{3\ Mes}$), 18.3 (C*H*$_{3\ Mes}$). HRMS (ESI): *m/z* calcd. for **[**$C_{42}H_{40}ClN_2ORu]^+$ ([M – $SbF_6]^+$) 725.1867, found 725.1878; ε_r = 1.5 ppm. IR 423, 443, 501, 534, 555, 584, 610, 619, 640, 653, 703, 713, 748, 754, 854, 915, 1031, 1049, 1098, 1180, 1216, 1233, 1386, 1446, 1469, 1566, 1584, 1607, 1962, 2328, 2616, 2920, 2972, 3084, 3147, 3183 cm^{-1}.

RCM of diethyl diallylmalonate (DEDAM)

A stock solution of DEDAM was prepared in the following manner: in a volumetric flask (5 mL), substrate (140 mg, 0.583 mmol) was weighed. Then, the flask was filled with toluene (dry, degassed). Next, the flask was closed with a rubber septum and shaken to homogenize the stock solution. This stock solution (600 µL) was introduced to the NMR tube equipped with a septum. The sample was equilibrated at 50 °C in the NMR probe. A stock solution of pre-catalyst was prepared in the following manner: pre-catalyst (3.5 µmol) was weighed in a volumetric flask (1 mL), then it was closed with the rubber septum and toluene(dry, degassed) (1 mL) was injected. An aliquot of the pre-catalyst (100 µL, 0.7 µmol) was taken from the stock solution and injected through the septum into a substrate solution in NMR tube. Data points were collected over an appropriate period using the Varian array function. The conversion of **4** was determined by comparing the ratio of the integrals of the methylene protons in the starting material, δH = 2.67 (s) with those in the product, δH = 2.98 (s). Yield was calculated according to the following equation: Yield (%) = ([P] × 100%)*/*([P]+[S]).

General procedure for the thermal stability studies

NMR tube was charged with a solution of Hoveyda-type pre-catalysts (12.8 µmol in toluene, 0.6 mL) and solution of 1,3,5-trimethoxybenzene (internal standard, 12.8 µmol in toluene, 0.1 mL). The sample was equilibrated at 50 °C. ^{1}H NMR spectra were measured after appropriate time intervals and the rate of pre-catalysts decomposition was monitored by the integration of protons of the internal standard at δ = 6.07 (s,3H) and the characteristic Ru=CH with chemical shifts around 17 ppm.

Crystallographic Experimental Details

The crystals were kept in their mother liquor until they were dipped into perfluoropolyether oil and their structure was determined. The chosen crystals were mounted on a Mitegen micromount with paratone-N oil and quickly cooled down to 100 K. For complexes **3a**, **3b**, **3c**, **7b**, and **14c**, the selected crystals were mounted on a Bruker Kappa APEX II using a micro-focus sealed X-ray tube, Mo-Kα radiation (λ = 0.71073Å) and equipped with an Oxford Cryosystems Cryostream Cooler Device. The structures have been solved by Direct Methods using SHELXS-97,[29] and refined by means of least-squares procedures on F^2 with either the aid of the program SHELXL2016**Erreur ! Signet non défini.** included in the software package WinGX version 1.63[30] or with the program CRYSTALS[31]. Absorption correction was done using multi-scan DENZO/SCALEPACK method.[32] The Atomic Scattering Factors were taken from International tables for X-Ray Crystallography.[33] All hydrogens atoms were placed geometrically and refined using a riding model. All non-hydrogens atoms were anisotropically refined, and in the last cycles of refinement a weighting scheme was used.

For complexes **6a** and **14b**, the selected crystals were mounted on an Agilent Technologies SuperNova Dual Source with the Cu*K*α radiation (*λ* = 1.54184 Å). The lattice parameters were obtained by least-squares fit to the optimized setting angles of the reflections collected by using the CrysAlis CCD software.[34] Data were reduced using the CrysAlis RED program. The analytical numeric absorption correction using a multifaceted crystal model based on expressions derived by R.C. Clark & J.S. Reid was applied.[35] The structural determination procedure was carried out using the SHELX package. The structure was solved with direct methods, and then successive least-squares refinements were carried out based on full-matrix least-squares on F^2 using the SHELXL program.[29] All H-atoms were positioned geometrically with the C−H bond length equal to 0.93, 0.96, 0.97 and 0.98 Å for the aromatic, methyl, methylene and methine H-atoms, respectively and constrained to ride on their parent atoms with *U*iso(H) = x*U*eq(C), where x = 1.2 for the aromatic, methylene and methine H-atoms, and 1.5 for the methyl H-atoms, respectively. Deposition Numbers 2249558 (**14c**), 2249559 (**3a**), 2249560 (**3b**), 2249561 (**7b**), 2249562 (**6a**), 2249563 (**14b**), and 2249564 (**3c**) contain the supplementary crystallographic data for this paper. These data are provided free of charge by the joint Cambridge crystallographic Data Centre and Fachinformationszentrum Karlsruhe Access Structures service www.ccdc.cam.ac.uk/structures.

Computational details

In this study we used a computational similar to our previous investigations of similar systems.[36] In short, geometry optimizations were carried out without constraints, and the characterization of stationary points was performed by analytical frequency calculations at the B3LYP/LACVP** level of theory.[37] The Gibbs free energies used throughout this study are the sum of electronic energy (M06-D3/LACV3P++**//B3LYP-D3/LACVP**), solvation energy (single-point Poisson–Boltzmann self-consistent polarizable continuum method in dichloromethane), zero-point energy correction, thermal correction to enthalpy, and the negative product of temperature and entropy, all at 298 K.[38] The M06 functional already includes medium-range dispersion, so M06-D3 can overestimate the effect of dispersion due to the double-counting of these effects.[39] On the other hand, the addition of D3 correction to M06 was shown to improve the results for many organic reactions, particularly in the treatment of weak interactions.[40] In all instances, standard convergence criteria and a ultrafine grid for DFT calculations were used, as implemented in Jaguar ver. 9.5.[41] Barriers for fluorenyl group rotations ($\mathbf{TS}_{\mathbf{3c\text{-}3c'}}$ and $\mathbf{TS}_{\mathbf{15c\text{-}15c'}}$) were estimated based on rotational scans along the N-C bonds in **3c** and **15c**.

Acknowledgements

This work was supported by the Centre National de la Recherche Scientifique (CNRS) and the University of Warsaw. The French Governement is gratefully acknowledged for an exchange program “Partenariat Hubert Curien” (PHC) Polonium and for part of a PhD grant to K. G.

Keywords: Ruthenium • N-heterocyclic Carbene • Cyclometalation • Olefin Metathesis • Migration

[1] a) Olefin Metathesis: Theory and Practice (Ed.: K. Grela), Wiley, Hoboken, 2014; b) Handbook of Metathesis (Eds.: R. H. Grubbs, A. G. Wenzel, D. J. O’Leary, E. Khosravi), Wiley-VCH, Weinheim, 2015.

[2] M. J. Benedikter, F. Ziegler, J. Groos, P. M. Hauser, R. Schowner, M. R. Buchmeiser, *Coord. Chem. Rev.* **2020**, *415*, 213315.

[3] (a) O. M. Ogba, N. C. Warner, D. J. O'Leary, R. H. Grubbs, *Chem. Soc. Rev.* **2018**, *47*, 4510-4544; (b) G. C. Vougioukalakis, R. H. Grubbs, *Chem. Rev.* **2009**, *110*, 1746-1787; (c) C. Samojłowicz, M. Bieniek, K. Grela, *Chem. Rev.* **2009**, *109*, 3708-3742.

[4] K. M. Dawood, K. Nomura, *Adv. Synth. Catal.* **2021**, *363*, 1970-1997.

[5] S. J. Meek, R. V. O/'Brien, J. Llaveria, R. R. Schrock, A. H. Hoveyda, *Nature* **2011**, *471*, 461-466.

[6] (a) K. Endo, R. H. Grubbs, *J. Am. Chem. Soc.* **2011**, *133*, 8525-8527; (b) B. K. Keitz, K. Endo, P. R. Patel, M. B. Herbert, R. H. Grubbs, *J. Am. Chem. Soc.* **2011**, *134*, 693-699; (c) P. Liu, X. Xu, X. Dong, B. K. Keitz, M. B. Herbert, R. H. Grubbs, K. N. Houk, *J. Am. Chem. Soc.* **2012**, *134*, 1464-1467; (d) S. M. Bronner, M. B. Herbert, P. R. Patel, V. M. Marx, R. H. Grubbs, *Chem. Sci.* **2014**, *5*, 4091-4098; (e) M. B. Herbert, R. H. Grubbs, *Angew. Chem. Int. Ed.* **2015**, *54*, 5018-5024; (f) M. B. Herbert, B. A. Suslick, P. Liu, L. Zou, P. K. Dornan, K. N. Houk, R. H. Grubbs, *Organometallics* **2015**, *34*, 2858-2869; (g) A. Dumas, R. Tarrieu, T. Vives, T. Roisnel, V. Dorcet, O. Baslé, M. Mauduit, *ACS Catal.* **2018**, *8*, 3257-3262; (h) Y. Xu, J. J. Wong, A. E. Samkian, J. H. Ko, S. Chen, K. N. Houk, R. H. Grubbs, *J. Am. Chem. Soc.* **2020**, *142*, 20987-20993.

[7] (a) G. Occhipinti, F. R. Hansen, K. W. Törnroos, V. R. Jensen, *J. Am. Chem. Soc.* **2013**, *135*, 3331-3334; (b) G. Occhipinti, V. Koudriavtsev, K. W. Tornroos, V. R. Jensen, *Dalton Trans.* **2014**, *43*, 11106-11117; (c) G. Occhipinti, K. W. Törnroos, V. R. Jensen, *Organometallics* **2017**, *36*, 3284-3292; (d) W. Smit, J. B. Ekeli, G. Occhipinti, B. Woźniak, K. W. Törnroos, V. R. Jensen, *Organometallics* **2020**, *39*, 397-407.

[8] (a) R. K. M. Khan, S. Torker, A. H. Hoveyda, *J. Am. Chem. Soc.* **2013**, *135*, 10258-10261; (b) A. M. Johns, T. S. Ahmed, B. W. Jackson, R. H. Grubbs, R. L. Pederson, *Org. Lett.* **2016**, *18*, 772-775; (c) M. J. Koh, R. K. M. Khan, S. Torker, M. Yu, M. S. Mikus, A. H. Hoveyda, *Nature* **2015**, *517*, 181-186.

[9] D. S. Müller, O. Baslé, M. Mauduit, *Beilstein J. Org. Chem.* **2018**, *14*, 2999-3010.

[10] L. Benhamou, S. Bastin, N. Lugan, G. Lavigne, V. César, *Dalton Trans.* **2014**, *43*, 4474-4482.

[11] (a) P. I. Jolly, A. Marczyk, P. Małecki, O. Ablialimov, D. Trzybiński, K. Woźniak, S. Osella, B. Trzaskowski, K. Grela, *Chem. Eur. J.* **2018**, *24*, 4785-4789; (b) P. I. Jolly, A. Marczyk, P. Małecki, D. Trzybiński, K. Woźniak, A. Kajetanowicz, K. Grela, *Catalysts* **2020**, *10*, 599.

[12] (a) M. Teci, E. Brenner, D. Matt, C. Gourlaouen, L. Toupet, *Dalton Trans.* **2014**, *43*, 12251-12262; (b) M. Teci, E. Brenner, D. Matt, C. Gourlaouen, L. Toupet, *Dalton Trans.* **2015**, *44*, 9260-9268; (c) M. Teci, E. Brenner, D. Matt, C. Gourlaouen, L. Toupet, *Chem. Eur. J.* **2015**, *21*, 10997-11000; (d) M. Teci, D. Hueber, P. Pale, L. Toupet, A. Blanc, E. Brenner, D. Matt, *Chem. Eur. J.* **2017**, *23*, 7809-7818.

[13] Deposition Numbers 2249558 (14c), 2249559 (3a), 2249560 (3b), 2249561 (7b), 2249562 (6a), 2249563 (14b), and 2249564 (3c) contain the supplementary crystallographic data for this paper. These data are provided free of charge by the joint Cambridge crystallographic Data Centre and Fachinformationszentrum Karlsruhe Access Structures service www.ccdc.cam.ac.uk/structures.

[14] A. W. Addison, T. N. Rao, J. Reedijk, J. van Rijn, G. C. Verschoor, J. *Chem. Soc., Dalton Trans. 1***984,** 1349-1356.

[15] M. Dąbrowski, P. Wyrębek, D. Trzybiński, K. Woźniak, K. Grela, C*hem. Eur. J. 2***020,** 2*6,* 3782-3794.

[16] (a) T. Ritter, A. Hejl, A. G. Wenzel, T. W. Funk, R. H. Grubbs, O*rganometallics 2***006,** 2*5,* 5740-5745; (b) M. Bieniek, A. Michrowska, D. L. Usanov, K. Grela, C*hem. Eur. J. 2***008,** 1*4,* 806-818.

[17] (a) S. Gupta, V. R. Sabbasani, S. Su, D. J. Wink, D. Lee, A*CS Catal. 2***021,** 1*1,* 1977-1987; (b) D. R. Anderson, D. D. Hickstein, D. J. O'Leary, R. H. Grubbs, J. *Am. Chem. Soc. 2***006,** 1*28,* 8386-8387.

[18] M. B. Herbert, Y. Lan, B. K. Keitz, P. Liu, K. Endo, M. W. Day, K. N. Houk, R. H. Grubbs, J. *Am. Chem. Soc. 2***012,** 1*34,* 7861-7866.

[19] A. K. Chatterjee, T.-L. Choi, D. P. Sanders, R. H. Grubbs, J. *Am. Chem. Soc. 2***003,** 1*25,* 11360-11370.

[20] A. H. Hoveyda, Z. Liu, C. Qin, T. Koengeter, Y. Mu, A*ngew. Chem. Int. Ed. 2***020,** 5*9,* 22324-22348.

[21] (a) C. J. Yue, Y. Liu, R. He, J. *Mol. Catal. A: Chem. 2***006,** 2*59,* 17-23; (b) J. Pollini, W. M. Pankau, L. J. Gooßen, C*hem. Eur. J. 2***019,** 2*5,* 7416-7425.

[22] (a) K. Endo, R. H. Grubbs, D*alton Trans. 2***016,** 4*5,* 3627-3634; (b) A. M. McKinty, C. Lund, D. W. Stephan, O*rganometallics 2***013,** 3*2,* 4730-4732; (c) B. Autenrieth, W. Frey, M. R. Buchmeiser, C*hem. Eur. J. 2***012,** 1*8,* 14069-14078; (d) O. Songis, A. M. Z. Slawin, C. S. J. Cazin, C*hem. Commun. 2***012,** 4*8,* 1266-1268; (e) M. Zirngast, E. Pump, A. Leitgeb, J. H. Albering, C. Slugovc, C*hem. Commun. 2***011,** 4*7,* 2261-2263; (f) M. A. O. Volland, S. M. Hansen, F. Rominger, P. Hofmann, O*rganometallics 2***004,** 2*3,* 800-816; (g) A. Fürstner, M. Liebl, C. W. Lehmann, M. Picquet, R. Kunz, C. Bruneau, D. Touchard, P. H. Dixneuf, C*hem. Eur. J. 2***000,** 6*,* 1847-1857.

[23] J. O. Krause, S. Lubbad, O. Nuyken, M. R. Buchmeiser, A*dv. Synth. Catal. 2***003,** 3*45,* 996-1004.

[24] (a) Z. Li, P. Ji, J.-P. Cheng, J. *Org. Chem. 2***021,** 8*6,* 2974-2985; (b) Z. Wang, Q.-H. Niu, X.-S. Xue, P. Ji, J. *Org. Chem. 2***020,** 8*5,* 13204-13210; (c) R. Schuldt, J. Kästner, S. Naumann, J. *Org. Chem. 2***019,** 8*4,* 2209-2218; (d) S. Naumann, C*hem. Commun. 2***019,** 5*5,* 11658-11670; (e) A. Doddi, M. Peters, M. Tamm, C*hem. Rev. 2***019,** 1*19,* 6994-7112; (f) M. M. D. Roy, E. Rivard, A*cc. Chem. Res. 2***017,** 5*0,* 2017-2025.

[25] (a) I. C. Watson, Y. Zhou, M. J. Ferguson, E. Rivard, Z. *Anorg. Allg. Chem. 2***022,** 6*48,* e202200082; (b) S. Ando, A. Ohara, T. Ohwada, T. Ishizuka, O*rganometallics 2***021,** 4*0,* 3668-3677; (c) I. C. Watson, A.

Schumann, H. Yu, E. C. Davy, R. McDonald, M. J. Ferguson, C. Hering-Junghans, E. Rivard, C*hem. Eur. J. 2***019,** 2*5,* 9678-9690; (d) K. Powers, C. Hering-Junghans, R. McDonald, M. J. Ferguson, E. Rivard, P*olyhedron 2***016,** 1*08,* 8-14; (e) D. A. Imbrich, W. Frey, S. Naumann, M. R. Buchmeiser, C*hem. Commun. 2***016,** 5*2,* 6099-6102; (f) M. Iglesias, A. Iturmendi, P. J. Sanz Miguel, V. Polo, J. J. Pérez-Torrente, L. A. Oro, C*hem. Commun. 2***015,** 5*1,* 12431-12434; (g) O. Esposito, D. E. Roberts, F. G. N. Cloke, S. Caddick, J. C. Green, N. Hazari, P. B. Hitchcock, E*ur. J. Inorg. Chem. 2***009,** 2*009,* 1844-1850; (h) A. Fürstner, M. Alcarazo, R. Goddard, C. W. Lehmann, A*ngew. Chem. Int. Ed. 2***008,** 4*7,* 3210-3214; (i) N. Kuhn, H. Bohnen, D. Bläser, R. Boese, C*hem. Ber. 1***994,** 1*27,* 1405-1407.

[26] A. J. Arduengo III, F. P. Gentry, Jr., P. K. Taverkere, H. E. Howard III, US Patent 6177 575, **2001**.

[27] G. R. Fulmer, A. J. M. Miller, N. H. Sherden, H. E. Gottlieb, A. Nudelman, B. M. Stoltz, J. E. Bercaw, K. I. Goldberg, O*rganometallics 2***010,** *29,* 2176-2179.

[28] L. E. Rosebrugh, M. B. Herbert, V. M. Marx, B. K. Keitz, R. H. Grubbs, J. *Am. Chem. Soc. 2***013,** 1*35,* 1276-1279.

[29] G. M. Sheldrick, *Acta Crystallogr., Sect. A: Found. Crystallogr*. **2008**, *64*, 112-122

[30] L. Farrugia, *J. Appl. Crystallogr.* **1999**, *32*, 837-838

[31] P.W. Betteridge, J.R. Carruthers, K. Prout, D.J. Watkin, *J. Appl. Cryst*. **2003**, *36*, 1487.

[32] R. Blessing, *Acta Crystallogr., Sec. A*. **1995**, *51*, 33

[33] INTERNATIONAL tables for X-Ray crystallography, **1974**, Vol IV, Kynoch press, Birmingham, England

[34] CrysAlis CCD and CrysAlis RED, Oxford Diffraction, Oxford Diffraction Ltd: Yarnton, **2008**.

[35] R. C. Clark, J. S. Reid, *Acta Crystallogr. A* **1995**, *51*, 887-897.

[36] (a) K. Młodzikowska-Pieńko, B. Trzaskowski, *Organometallics* **2022**, *41*, 3627-3635.(b) S. Planer, P. Małecki, B. Trzaskowski, A. Kajetanowicz, K. Grela, *ACS Catal.* **2020**, *10*, 11394-11404. (c) M. Jawiczuk, A. Marczyk, K. Młodzikowska-Pieńko, B. Trzaskowski, *J. Phys. Chem. A* **2020**, *124*, 6158-6167.(d) P. Małecki, K. Gajda, R. Gajda, K. Woźniak, B. Trzaskowski, A. Kajetanowicz, K. Grela, *ACS Catal.* **2019**, *9*, 587-598. (e) R. Gawin, A. Tracz, M. Chwalba, A. Kozakiewicz, B. Trzaskowski, K. Skowerski, *ACS Catal.* **2017**, *7*, 5443-5449.

[37] (a) A. D. Becke, *J. Chem. Phys.* **1993**, *98*, 5648-5652.(b) C. Lee, W. Yang and R. G. Parr, *Phys. Rev. B* **1988**, *37*, 785-789

[38] Y. Zhao, D. G. Truhlar, *Theor. Chem. Acc.* **2008**, *120*, 215-241

[39] L. Goerigk, *J. Phys. Chem. Lett.* **2015**, *6*, 3891-3896

[40] S. Luo, Y. Zhao, D. G. Truhlar, *Phys. Chem. Chem. Phys.* **2011**, *13*, 13683-13689

[41] A. D. Bochevarov, E. Harder, T. F. Hughes, J. R. Greenwood, D. A. Braden, D. M. Philipp, D. Rinaldo, M. D. Halls, J. Zhang, R. A. Friesner, *Int. J. Quantum Chem.* **2013**, *113*, 2110-2142.